



Smart Polymer Fibers: Promising Advances in Microstructures, Stimuli-Responsive Properties and Applications

Yiling Yu¹ · Fenghua Zhang¹ · Yanju Liu² · Jinsong Leng¹

Received: 1 November 2024 / Accepted: 3 March 2025
© Donghua University, Shanghai, China 2025

Abstract

The advancement of fiber materials over the centuries has played a crucial role in the progress of human civilization. Smart polymer fibers (SPFs) are a revolutionary family of materials with sensory, feedback, and responsive attributes to chemical and physical stimuli, and are characterized by diverse microscopic structures. Multidimensional fiber microstructures have been fabricated by sophisticated preparation technologies, such as electrospinning, wet spinning, and microfluidic spinning, resulting in SPFs with responsiveness to various stimuli, such as thermal, pH, light, electricity, moisture, magnetic field, and multiple stimuli-responsive properties. In the past decade, cross-disciplinary developments in the refinement, intellectualization, and functionalization of SPFs and notable progress in the fibers' microstructure and stimuli-responsive properties have enabled wide applications in biomedicine, smart textiles, sensors, and water treatment. Herein, to comprehensively facilitate SPFs development in multidisciplinary and multifunctional domains, we elaborate on the correlation among material classification, microstructures formed by common preparation processes, stimuli-responsive properties, and their comprehensive applications. Finally, we aim to inspire scientists with diverse research backgrounds to apply multidisciplinary knowledge to promote the development and industrialization of SPFs.

Keywords Smart polymer fibers · Microstructure · Stimuli-responsive properties · Applications

1 Introduction

Fibers have long been utilized throughout the course of human civilization, and they have been accompanied by the development of fibrous materials [1]. Smart polymer fibers (SPFs) are promising smart materials that have been extensively researched and used in the disciplines of biomedicine [2, 3], smart sensors [4], and smart textiles [5, 6], owing to their unique stimulus-responsive properties, excellent mechanical performance, and tunable physicochemical characteristics. SPFs can detect changes in their internal or

external surroundings and respond actively via internal or feedback mechanisms [7, 8]. In particular, SPFs are characterized by the following properties: (1) sensing functionality to detect the intensity of internal stimuli, such as thermal [9–11], light [12, 13], pH [14], electricity [15], moisture [16, 17], magnetic field [18], multiple stimuli-responsive properties [19, 20]; (2) a driving function and the ability to respond to environmental changes; (3) the ability to select and control the response in a programmable manner; (4) a sufficiently sensitive, timely, and appropriate response for the intended application; and (5) quickly return to the original state when the stimuli-responsive properties are eliminated [21].

Fabricating a multidimensional microstructure with the morphology characteristic of SPFs is a crucial strategy in the field of modern materials science, and the microstructures of SPFs with a wide variety of functions are typically fabricated by electrospinning, wet spinning, or microfluidic spinning technology. By carefully designing and manipulating fiber microstructures, such as hollow fibers, microbelt fibers [22], wrinkled fibers [23], and core-sheath fibers [15], their physical and chemical properties can be significantly

✉ Fenghua Zhang
fhzhang_hit@163.com

✉ Jinsong Leng
lengjs@hit.edu.cn

¹ Centre for Composite Materials and Structures, Harbin Institute of Technology (HIT), No. 2 Yikuang1 Street, Harbin 150080, People's Republic of China

² Department of Astronautic Science and Mechanics, Harbin Institute of Technology (HIT), No. 92 West Dazhi Street, Harbin 150001, People's Republic of China

altered to meet the needs of various application scenarios. For example, the introduction of hollow channels increases the specific surface area and load-bearing capacity of micro-fibers [22]. SPFs can respond to various environmental changes, thereby showing great application prospects in the fields of cell growth [24], drug delivery [25], tissue regeneration [26], smart sensors [27], smart textiles, color-changing fibers [28], water treatment [29] and others.

In this review, the major classifications and descriptions of polymers constructing SPFs in recent years are presented, and their fundamental principles and rich and

diverse microstructures are elaborated, thereby providing a theoretical and research foundation for the study of SPFs. The diverse stimuli-responsive properties of SPFs are influenced by their rich microscopic morphology. The wide range of applications, several domains, and inventive applications of SPFs emphasize their "smart" nature. Finally, the future development route of SPFs in application areas is outlined, providing new viewpoints and distinctive insights for future advancements, while considering the difficulties faced in expediting clinical applications and industrial production (Fig. 1).

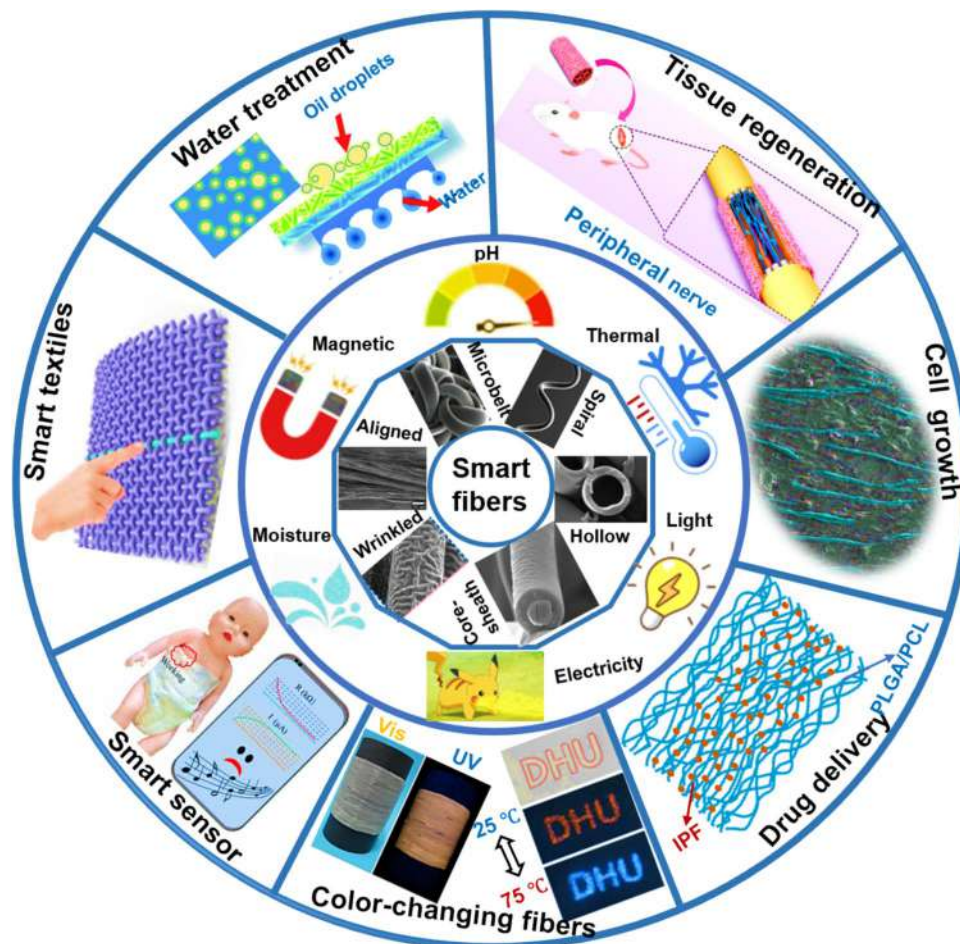


Fig. 1 Illustration of microstructures, stimuli-responsive properties and applications of SPFs. The structural diversity of SPFs is presented within the blue dodecagon, while the stimuli-responsive properties are presented outside it. The applications of SPFs are roughly classified into cell growth, drug delivery, tissue regeneration, color-changing fibers, smart textiles, smart sensors, water treatment, and others; Reproduced with permission from ref [22], Copyright 2011, Royal Society of Chemistry; Reproduced with permission from ref [23], Copyright 2023, Springer Nature; Reproduced with permission from ref [30], Copyright 2019, John Wiley and Sons; Reproduced with permission from ref [31], Copyright 2019, American Chemi-

cal Society. Reproduced with permission from ref [32], Copyright 2023, American Chemical Society; Reproduced with permission from ref [24], Copyright 2020, American Chemical Society; Reproduced with permission from ref [25], Copyright 2020, Elsevier; Reproduced with permission from ref [26], Copyright 2020, American Chemical Society; Reproduced with permission from ref [28], Copyright 2021, American Chemical Society; Reproduced with permission from ref [27], Copyright 2022, American Chemical Society; Reproduced with permission from ref [29], Copyright 2014, Royal Society of Chemistry

2 Smart Polymer Fibers

Based on the provision of a relatively clear framework and direction for development in the field of SPFs, this article classifies them into three major categories: shape memory fibers (SMFs), hydrogel fibers, and liquid crystal fibers (LCFs).

2.1 Shape Memory Fibers

Shape memory polymers (SMPs) are a class of smart materials that can undergo significant deformation from a temporary shape to a pre-programmed permanent shape upon exposure to an external stimulus. SMFs are fiber materials prepared through fiber processing technology based on SMPs. SMFs [33] are capable of reverting from temporary shapes (e.g., straight lines, waves) to their original shapes when subjected to specific external stimuli, thereby completing the shape memory cycle [34, 35]. Take thermal-responsive SMFs as an example (Fig. 2a). Typically, SMFs consist of a dual structure of fixed and reversible phases [33, 36]. The fixed phase is responsible for maintaining the

original fiber shape, whereas the reversible phase determines the shape-memory activation temperature of SMFs and the retention capacity of the temporary shape [37]. When SMFs are deformed by an external force and heated above their shape memory activation temperature, the polymer chains rearrange and return to their original state, thereby achieving complete shape recovery [38]. With the continuous advancement of smart polymer fibers, SMFs have transitioned from unidirectional shape memory to two-way SMFs and multiple SMFs, which can meet the complex applications in biomedicine, smart textiles, and other fields [39].

Two-way SMFs can reversibly transform between two predetermined shapes under the action of external stimuli. SMFs that can reversibly transform from one permanent shape into another are known as two-way SMFs or reversible SMFs [40]. Compared with the irreversible one-way shape memory process, two-way SMFs can switch between two shapes autonomously under different environmental conditions without artificial deformation. Therefore, two-way SMFs have great application prospects in biomedical applications, smart textiles, and smart sensors. [41].

Multiple SMFs can memorize and recover multiple temporary shapes in response to specific external stimuli

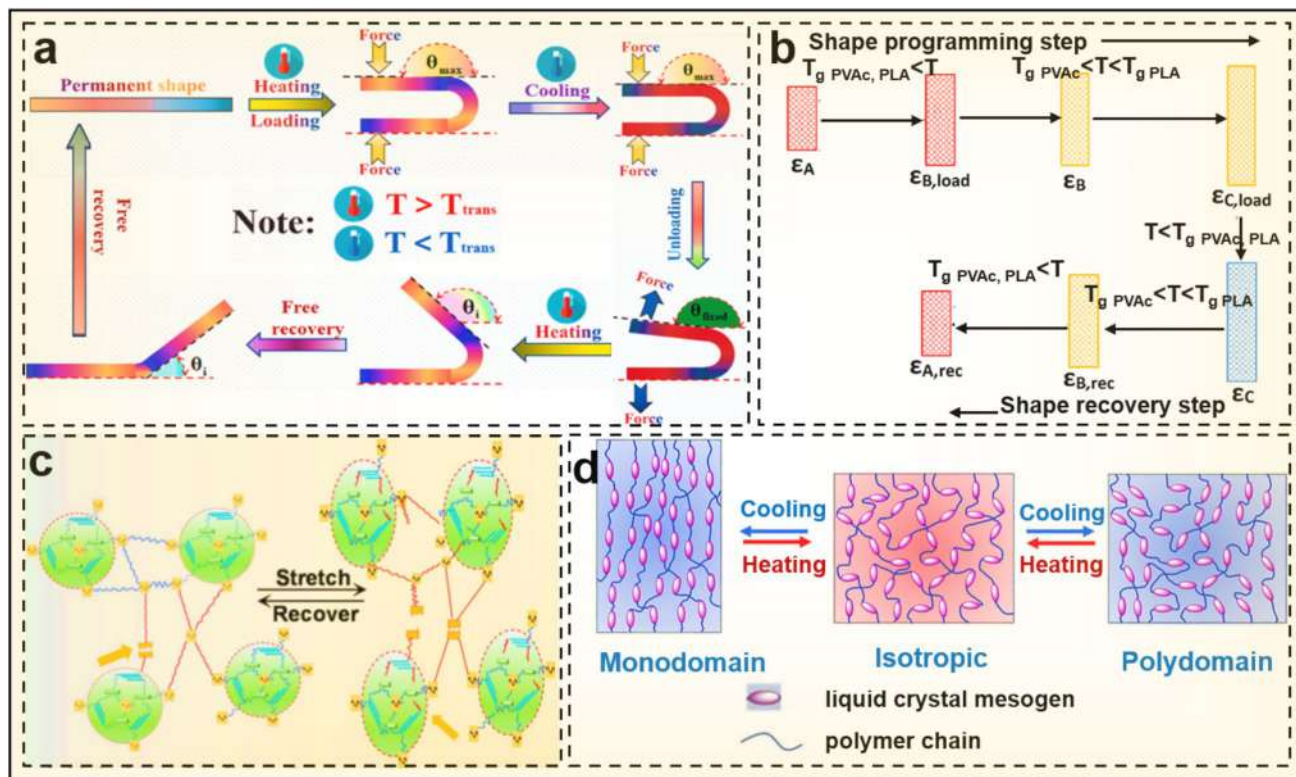


Fig. 2 Mechanism schematic diagram of three major categories of smart polymer fibers. **a** Schematic diagram of thermal-responsive SPFs; Reproduced with permission from ref [38]; Copyright 2022, Elsevier. **b** Schematic diagram of multiple SPFs; Reproduced with permission from ref [39], Copyright 2019, John Wiley and Sons. **c**

Hydrogen bonding of hydrogel fibers; Reproduced with permission from ref [47]; Copyright 2024, American Chemical Society. **d** The schematic illustration of the molecular structure of monodomain and polydomain LCEs; Reproduced with permission from ref [54]; Copyright 2023, Taylor and Francis

[42]. There are generally the following ways to realize the multi-shape memory effects: either by designing SMPs with a wide temperature transition range or by combining multi-component polymers with different glass-transition temperatures (Fig. 2b) [39]. Fixing different temporary shapes in multiple SMFs requires deformation at the corresponding interval transition temperatures, and this process is referred to as multi-step programming. Multiple SMFs with their unique characteristics provide new ideas and broad prospects for the in-depth development of the biomedical field and robots.

2.2 Hydrogel Fibers

Hydrogel fibers are a class of 3D network materials formed by the cross-linking of hydrophilic polymers. Due to its ability to automatically adjust its own properties or appearance under specific environmental changes, these materials achieve diversified applications for biomedicine, water treatment, and smart sensors [43]. Hydrogel fibers have the following main characteristics: (1) sensing changes in the external environment and converting this information into corresponding response signals; (2) automatically adjusting their structures and properties according to changes in the external environment to achieve the preset functions; (3) returning to their original state after the external stimuli disappear, enabling repeated use [44, 45]. Under specific environmental circumstances, hydrogel fibers exhibit multifunctional attributes, such as self-assembly [46], self-healing, and sensing, through the fine regulation of internal polymer chain interactions, such as hydrogen bonds and ionic bonds (Fig. 2c) [47]. Hydrogel fibers respond to environmental stimuli and change their properties, such as transparency, gel volume, mechanical adsorption/desorption, and surface, affecting their growth actions, network structure, and permeability [48]. Hydrogel fibers with this "sensing" property can undergo reversible volume phase transitions or sol–gel phase transitions when environmental conditions change [49].

2.3 Liquid Crystal Fibers

LCFs are among the most promising next-generation smart soft materials [50, 51]. The smart responses of LCFs are based on their molecular-level adjustability, which enables changes in their morphology or performance when exposed to external stimuli. The molecular structure and physical properties of liquid-crystal polymers enable distinctive performance. LC polymers are network structures formed through the chemical cross-linking of anisotropic LC monomers [52]. Under specific circumstances, these molecules exhibit ordered arrangements, forming an LC

phase that endows the material with unique optical and mechanical properties [53].

Liquid crystal elastomers (LCEs) are classified as single- or multidomain LCEs based on the arrangement of mesogenic LC units. In single-domain LCEs, the single-directional ordered arrangement of LC mesogenic units results in reversible and significant deformation during the phase transition. In multidomain LCEs, the randomly distributed LC domains result in an overall macroscopic ability to maintain the original shape, unlike single-domain LCEs that undergo significant deformation in only one direction (Fig. 2d) [54].

3 Fibers Microstructure Through Fabrication Strategies

3.1 Electrospinning Polymer Fibers

The construction of a multi-dimensional microstructure with diverse fiber morphologies constitutes a crucial strategy in the areas of modern materials science. Electrospinning (ESP) technology utilizes electrostatic forces [55] to create continuous fibers with diameters varying from a few nanometers to a few microns [34]. The ESP system is basic and primarily comprises a receiver, propeller, high-voltage power supply, and syringe pump (Fig. 3) [56]. Through the use of a variety of natural or synthetic polymers, ESP can produce nanofiber matrices with precise fiber placement and structural integrity [57].

As depicted in Fig. 3, aligned polycaprolactone (PCL) fibers loaded with particles facilitate cellular orientation [58], demonstrating an application direction for SPFs. Kebab-structured fibers have an innovative morphology that induces directed crystal growth, making them suitable for applications in smart sensors, tissue regeneration and nanoelectronics [59]. Shape memory polyurethane (SMPU) nanofibers with core–shell or bead-on-string structures exhibit excellent shape memory effects with antibacterial activity against certain bacteria [60]. Adjusting the size of SiO₂ particles during the preparation of polyvinyl alcohol (PVA)/SiO₂ fibers shows that particles with a diameter of 910 nm tend to be arranged sequentially along the fiber's axial direction [61]. Ultrathin three-layered core–shell fibers with microtube nanowire structures were fabricated by multifluid coaxial spinning, demonstrating the capacity of ESP to precisely control the material structure at the nanoscale [62].

Nanofibers with short branches were prepared using a 3 wt% aqueous PVA solution [63]. Furthermore, biomimetic Y-shaped microtubular fibers prepared by multifold compound jetting ESP exhibited controllable channel numbers, diameters, and internal morphologies, and the

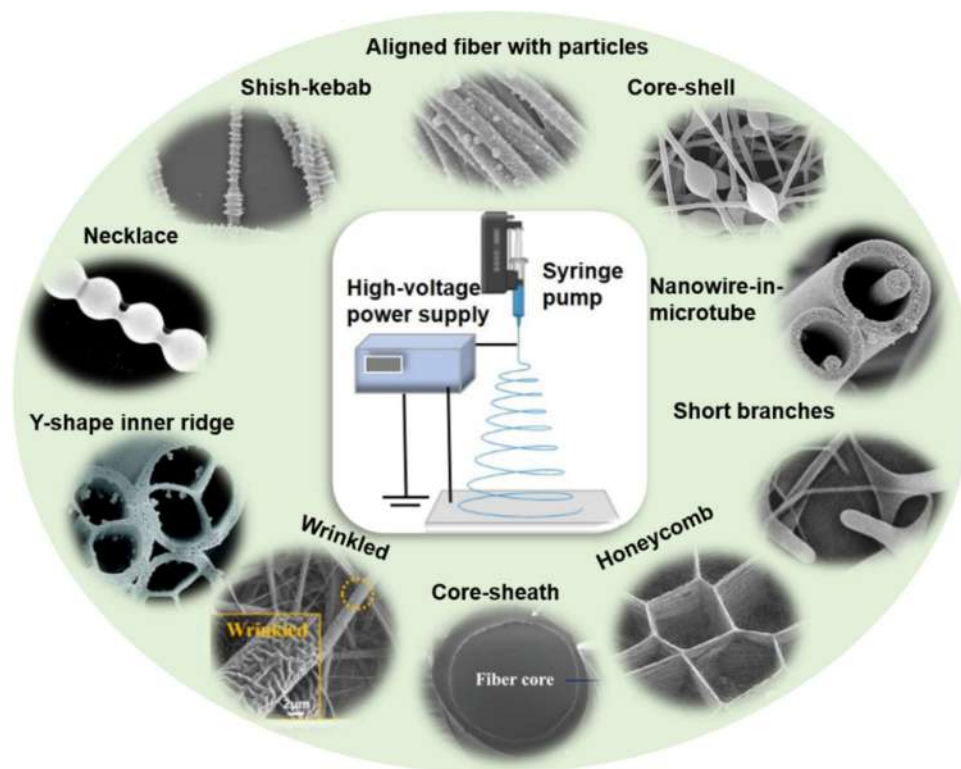


Fig. 3 Schematic diagram and scanning electron microscope (SEM) diagram of the basic device of ESP and its microstructure. Aligned PCL fiber with particles; Reproduced with permission from ref [58], Copyright 2022, John Wiley and Sons. The Shish kebab fiber; Reproduced with permission from ref [59], Copyright 2008, American Chemical Society. Core-shell fiber; Reproduced with permission from ref [60], Copyright 2011, BME-PT and GTE. The necklace fiber; Reproduced with permission from ref [61], Copyright 2010, American Chemical Society. The core-shell fibers with a nanowire-in-microtubule structure; Reproduced with permission from ref [62], Copyright 2010, American Chemical Society. The wrinkled structure

of PDDO/poly(L-lactide) (PLA) nanofibers; Reproduced with permission from ref [23], Copyright 2023, Springer Nature. Enlargement of the spikes extending from thin nanofibers for PVA short branch fibers spun from a 3 wt% aqueous solution; Reproduced with permission from ref [63], Copyright 2008, John Wiley and Sons. Y-shaped microtubular fibers; Reproduced with permission from ref [64], Copyright 2007 American Chemical Society. The core-sheath structure of LCFs; Reproduced with permission from ref [65], Copyright 2019, John Wiley and Sons. Structure of honeycomb fiber; Reproduced with permission from ref [67], Copyright 2011, American Chemical Society

authors proposed various application prospects [64]. Herein, three kinds of structures are distinguished according to the different conditions of the microstructure interface. The core-shell structure is an integrated double-layer structure that can be clearly distinguished; the core-sheath structure is an integrated double-layer structure that is fuzzy, and the sheath-core structure is a nonintegrated double-layer structure that can be distinguished.

Core-sheath LCFs with a black nylon monofilament coated with a low-molecular-weight LC and an outer sheath coated with polyvinylpyrrolidone (PVP) were stronger and showed a greater response to external stimuli than LC core fibers produced by ESP or spray guns [65]. During ESP, a mixture of LC polysiloxane solution with cholesterol side chains, small molecule LC, triethylamine, and polyethylene oxide (PEO) promotes strong interactions between LC polysiloxane and PEO molecules while enhancing the regular

arrangement of polymer molecules in the fibers, thereby forming LCFs with specific orientations [66].

The interaction between surface tension and electrostatic repulsive forces propels charged wet nanofibers during the self-assembly process of SPFs, resulting in honeycomb-patterned nanofiber structures of polyacrylonitrile (PAN), PVA, and PEO [67], which have a wide range of applications. Moreover, SMFs membranes that can achieve smart transformations between wrinkled and smooth morphologies have been produced through a shape-programming process of orienting and elongating polymer chains driven by electrostatic forces [23]. However, this process also has several drawbacks, including low spinning efficiency, the use of organic solvents, insufficient fiber strength, complex equipment, larger fiber diameter, material selection limitations, and low production yield, which limit its large-scale application and further development.

3.2 Wet Spinning Polymer Fibers

Wet spinning is an environmentally friendly spinning process that involves dissolving a polymer in a solvent and extruding it through spinning holes to solidify it into filaments in a coagulation medium [68]. The process consists of dissolution, extrusion, coagulation, and collection steps (Fig. 4a) [47]. Fine control of the microstructure of SPFs can be achieved by precisely controlling the process parameters, such as the concentration and molecular weight of the polymer, the composition and temperature of the solidification bath, and the size and shape of the spinneret [69].

The organic hydrogels in hydrogel fibers consisting of PVA, tetra aniline, ethylene glycol, and water have an inhomogeneous and fragile hydrogen bond network as a

pathway for ion transport to achieve ultralow detection limits and high tensile sensitivities (Fig. 4a) [47]. Furthermore, core-shell hydrogel fibers with the thermal-responsive properties containing a poly(3, 4-ethylene-dioxythiophene):poly(4-styrene sulfonate) (PEDOT:PSS) core and PU/graphene shell were fabricated by integrating wet spinning and impregnation technologies (Fig. 4b) [34]. As illustrated in Fig. 4c, the incorporation of a rotating collection bath in the traditional wet spinning process allows for the fabrication of hydrogel microfibers with submicron morphologies and promotes their automatic assembly, resulting in hierarchically aligned fibers at a macroscopic scale [70].

Computer-aided wet spinning enables the fabrication of diverse fiber scaffolds with varying shapes, sizes, porosities, and controllable two-scale porous structures (Fig. 4d) [69].

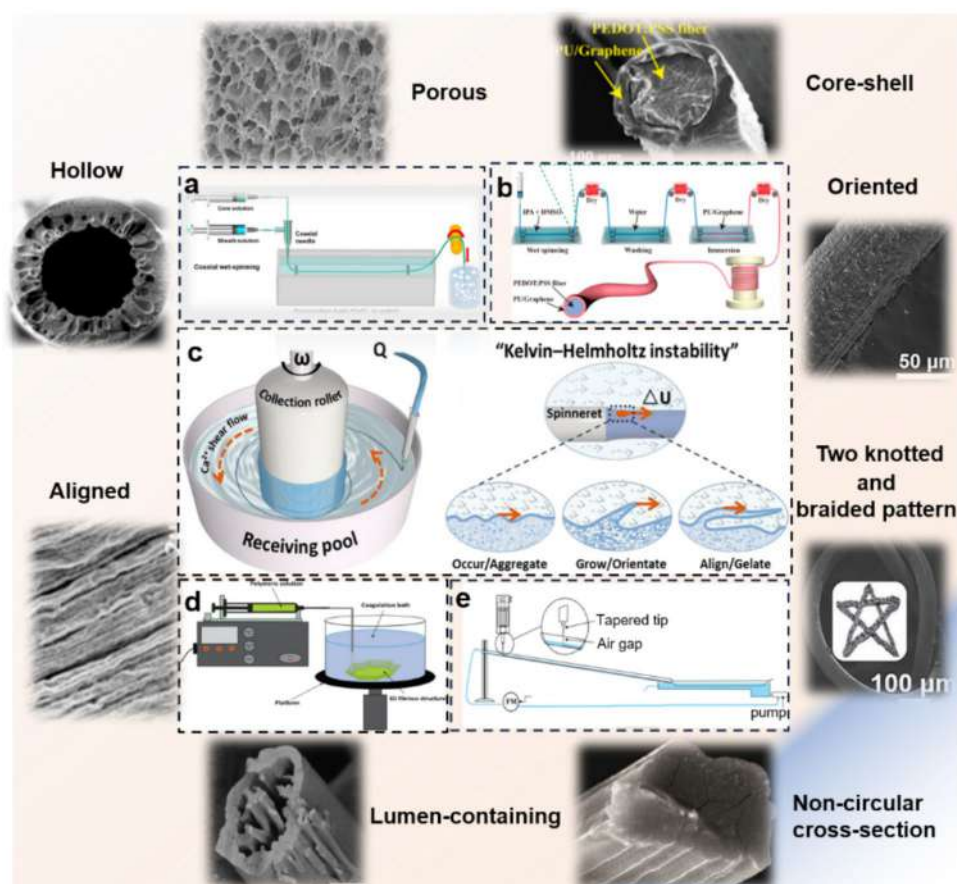


Fig. 4 **a** The coaxial wet spinning process and porous hydrogel fibers; Reproduced with permission from ref [47], Copyright 2024, American Chemical Society. **b** Schematic diagrams for fabricating core-shell hydrogel fibers; Reproduced with permission from ref [34], Copyright 2023, American Chemical Society. **c** The rotated wet spinning process and construction of the microstructure of aligned fibers; Reproduced with permission from ref [70], Copyright 2017, Oxford University Press. **d** Schematic diagrams of the computer-aided wet spinning process; Reproduced with permission from ref [69], Copyright 2022, Elsevier. **e** Schematic diagrams of the spinning line using

a deep eutectic solvent and an inclined channel; Reproduced with permission from ref [71], Copyright 2018, American Chemical Society. Oriented composite fiber, two knotted fibers, and a braided pattern; Reproduced with permission from ref [74], Copyright 2023, John Wiley and Sons. Lumen-containing and non-circular cross-sections of nanofibers; Reproduced with permission from ref [72], Copyright 2019, Elsevier. Hollow nanofibers; Reproduced with permission from ref [73], Copyright 2018, Molecular Diversity Preservation International

A modular spinning system with various ethanol flow, dope flow rate, channel, and spinning baths can be achieved for the continuous production of fiber yarn (Fig. 4e) [71]. The structures of lumen-containing and noncircular cross-sectional silk fibroin fibers were controlled by adjusting the concentrations of the spinning solution and coagulant, as well as the temperature [72]. Hollow polyether sulfone fibers were fabricated via dry-jet wet spinning by adding ethylene glycol and poly(sodium 4-styrene sulfonate) to the spinning dopes to make them permeable to water, thus expanding their potential applications in water treatment [73]. Ca^{2+} was employed as a crosslinking agent in an alginate solution to produce oriented composite fiber, knotted fibers, and braided liquid metal (LM)/alginate fibers [74].

Microfluidic technology, with its advantages of high precision, high throughput, ease of integration, and automation, enables the efficient fabrication of diverse fiber morphologies. However, its complex manufacturing processes, high costs, susceptibility to channel clogging, and stringent operational requirements have hindered the industrialization of this technology. In brief, wet spinning has unique advantages in constructing diverse fiber microstructures, and through continuous innovation and optimization, it can enable the fabrication of fiber microstructures to meet the specific needs of different applications and support the development of related industries.

3.3 Microfluidic Spinning Polymer Fibers

Microfluidic spinning technology has been used to design well-defined structures, controlled compositions, and organized functions in micro/nanoscale spun fibers. It allows chemical reactions to occur in a controlled manner at ultrasmall scales to achieve specific functions [75]. The microfluidic spinning system includes a microfluidic system (pump, microfluidic chip, and microfluidic needle), a high-voltage power supply, and an electronic control platform. In addition, microfibers with bilayer structures [76], spiral structures [77], triple structures, core-shell structures [78], and sheath-core structures [79] have been successfully generated by changing the injection capillary design of the microfluidics [80].

Double-hollow and microbelt hydrogel fibers were prepared from poly(ethylene glycol) diacrylate and n-hexadecane, using 2-hydroxy-2-methylpropiophenone as the photoinitiator, through a combination of polymeric jet streams and in situ photopolymerization (Fig. 5) [22]. The rapid and continuous self-assembly of internal cellulose nanocrystals is facilitated by the formation of a hydrogel sheath as a protective shield to form multilayer ultra-LCFs with a core-sheath structure [81]. *E. coli* cells were introduced into an aqueous solution of sodium alginate to produce hydrogel

fibers with a sheath-core structure, allowing the free transport of small molecule nutrients or targets while providing a segregated environment for cell growth [79]. Programmable spindle knots were formed by subjecting the jet of the pre-gel solution flowing in the channel to a programmable piezoelectric signal, which induces rapid polymerization of wavy jets, resulting in uniform, gradient, and symmetrical knot structures [82]. Droplets inside the fiber channels can form capillary bridges using a multiphase laminar flow microfluidic strategy. The partitioning properties of a dual aqueous phase were applied to prepare periodic spindle microfibers with a continuous hollow structure for water applications [83].

The advantages of microfluidic spinning are that it can accurately control the size, structure, and composition of fibers, and the spinning process is stable and repeatable. However, it faces challenges such as high process control difficulty, poor stability, and limited fiber diameter range.

4 Stimuli-Responsive Properties

SPFs are capable of "sensing" different physical and chemical stimuli and "responding" to one or more of their properties [84]. SPFs allow them to respond to minute changes in environmental conditions, endowing these materials with broad application prospects in the fields of biomedicine, smart textiles, sensors, and water treatment.

4.1 Thermal-Responsive Properties

Thermal-responsive polymer fibers, or temperature-responsive polymer fibers, are fiber materials that can undergo corresponding morphological modifications with temperature changes. The central property of these fibers is that their polymer chains undergo a shift between two thermodynamically stable states in solution, which is directly affected by temperature [85]. Core-shell SMFs with an epoxy resin core and PCL shell achieved rapid shape-memory recovery in only 6.2 s at 70 °C, demonstrating efficient thermal-responsive properties and highlighting their potential for multidomain applications [86]. Nanofibers mixed with plasticized PLA and lactate oligomers were processed by ESP to obtain heat-activated SMFs [87]. The shape memory properties were observed at a glass-transition temperature close to human body temperature, demonstrating their potential for use in biomedical applications. Furthermore, the performance of a thermal-responsive PU biomimetic fiber scaffold was optimized by manipulating the macro/microstructure of the fibers [88].

Hollow nanofibers hydrogels (HNFHs) were synthesized by radical copolymerization of *N*-isopropylacrylamide and *N*-methylacetamide (NMA) to prepare thermal-responsive

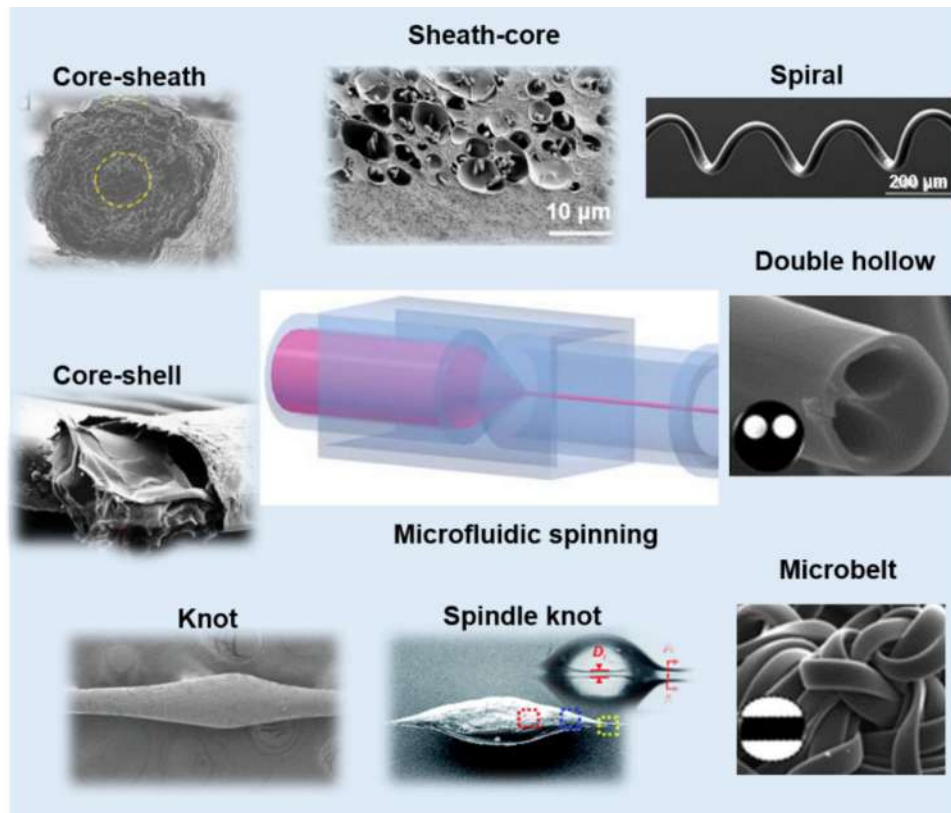


Fig. 5 Schematic diagram of microfluidic spinning and the microstructure of a spiral fiber; Reproduced with permission from ref [30], Copyright 2019, John Wiley and Sons. Double hollow fiber and microbelt fibers; Reproduced with permission from ref [22], Copyright 2011, Royal Society of Chemistry. Core-shell microfibers; Reproduced with permission from ref [78], Copyright 2019, John Wiley and Sons. Core-shell hydrogel fibers; Reproduced with permission from ref [76], Copyright 2019, John Wiley and Sons.

The sheath-core hydrogel fibers; Reproduced with permission from ref [79], Copyright 2023, John Wiley and Sons. The core-sheath structure of LCE fibers; Reproduced with permission from ref [81], Copyright 2020, John Wiley and Sons. Knot fibers; Reproduced with permission from ref [82], Copyright 2021, John Wiley and Sons. Spindle-knotted microfibers; Reproduced with permission from ref [83], Copyright 2022, Royal Society of Chemistry

polymers with a hollow structure After freeze-drying, the HNFHs based on the thermal-responsive polymers were heated to generate crosslinking points and chemical bonds, rendering high stability in water (Fig. 6a) [9]. Its multiple porous structures facilitated water diffusion during the temperature-induced volume phase transition, and the response time was less than 30 s. Ultrafast HNFH-2 could respond to temperature changes ranging from 15 to 47 °C, enabling "on-off" switchable release of drugs, which shows its potential as an implantable macroscopic drug delivery system. As shown in Fig. 6b, the porous structure of PLA/polydioxanone (PPDO) SMFs showed a disordered arrangement and folded surface properties [23]. Horizontal stretching at 42 °C promoted the directional arrangement of the fibers, reducing the internal porosity and unfolding the fiber surfaces to generate a smoother appearance After shape restoration, the fibers returned to a nondirectional state, and the original porous structure and folded surface

were restored Biodegradable poly(d, l-lactide-co-trimethyl carbonate) (PLMC) nanofiber membranes prepared by ESP were tested in spiral and cylindrical rod shapes (Fig. 6c) [89]. The shape recovery of the thermal-responsive SMFs samples in "SMP" shapes were completed within 12 s, and a typical shape recovery process was observed at 39 °C.

As illustrated in Fig. 6d, chiral cholesterol liquid crystals encapsulated in a black nylon monofilament core exhibited multicolored reflective properties at room temperature, with blue, red, and green spectra [65]. As the temperature was increased to 55 °C, the reflective properties of the red and green bands changed significantly; the red color changed to invisible infrared radiation (which appeared black), and the green color changed to red When the temperature reached 70 °C, the color reflection of all visible light bands disappeared and was converted into infrared radiation, resulting in a uniform black appearance on the textile's surface,

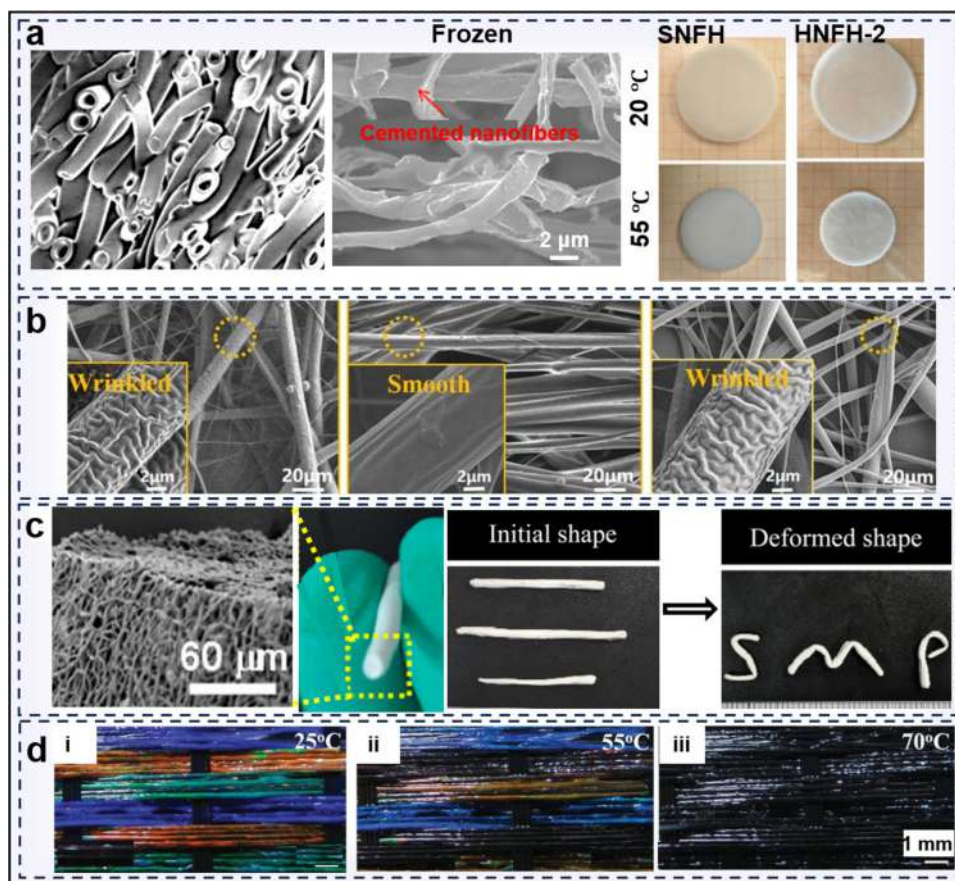


Fig. 6 **a** SEM of the cross-sections and the precursors of the prepared HNFH with super-elasticity. Optical images of solid nanofibrous hydrogel (SNFH) and HNFH-2 in water at 20 °C (up) and 55 °C (down); Reproduced with permission from ref [9], Copyright 2020, John Wiley and Sons. **b** PLA/PPDO SMFs and corresponding SEM

images; Reproduced with permission from ref [23], Copyright 2023, Springer Nature. **c** Shape memory PLMC fibers; Reproduced with permission from ref [89], Copyright 2014, American Chemical Society. **d** (i–iii) LCL fiber color at different temperatures; Reproduced with permission from ref [65], Copyright 2019, John Wiley and Sons

reflecting the optical response mechanism of the LCL fiber with temperature.

4.2 pH-Responsive Properties

Over the past few decades, pH-responsive polymer fibers have attracted considerable research attention because of their broad range of applications [48]. pH-responsive polymer fibers are a class of intelligent fibrous materials capable of exhibiting specific responses (such as shape changes, volume expansion or contraction, color changes, etc.) to variations in environmental pH [90]. Encapsulating pH-responsive dyes within hydrogel fibers not only prevents the dyes from dispersing into the wound area but also provides a biocompatible interface with the wound site. Additionally, pH values can be determined through images directly captured by smartphones, offering convenience for health monitoring in daily life (Fig. 7a) [91].

pH-responsive polymer fibers with a core–shell structure can control the rate and amount of drug delivery through micromorphology in response to pH changes. The introduction of acid-reactive ibuprofen-loaded sodium bicarbonate into the poly-L-lactic acid (PLLA) fiber scaffold has been designed to prevent minor inflammation and promote regeneration (Fig. 7b) [92]. The acid-responsive fibrous scaffold displayed rapid drug release at pH 5.0 and sustained drug release at pH 7.4. As shown in Fig. 7c, PVA/PAA-epigallocatechin gallate (EGCG) can reversibly swell (pH > 7.4) and shrink (pH < 6.5) in response to pH, thereby controlling drug release rates and dynamically regulating the intricate inflammatory wound environment [93].

Nanofibers are employed as particle carriers for pH-responsive structures [90]. These particles can change their properties in response to different pH, enabling the controlled release of drugs or other substances. As shown in Fig. 7d, a model peptide was efficiently encapsulated under mild conditions, and the nanocarriers were further

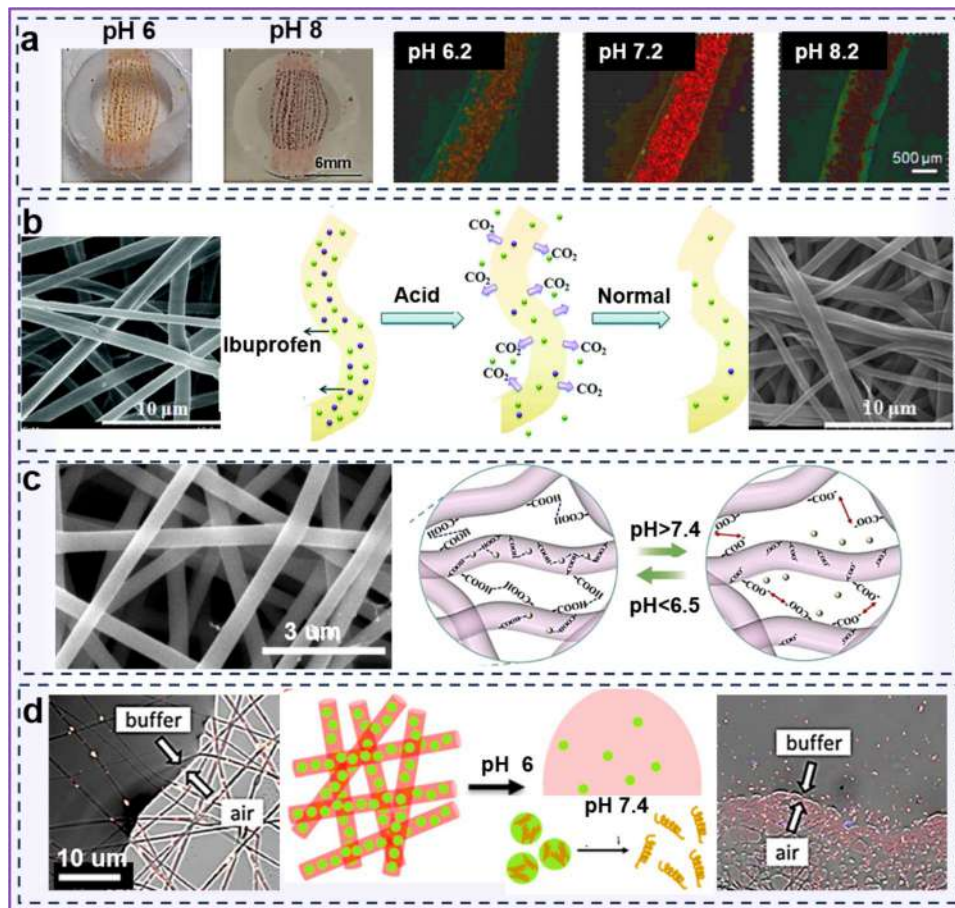


Fig. 7 **a** The hydrogel fibers containing microbeads that respond to different pH-responsive properties; Reproduced with permission from ref [91], Copyright 2016, John Wiley and Sons. **b** The acid-responsive ibuprofen-loaded PLLA fibrous scaffolds; Reproduced with permission from ref [92], Copyright 2014, Royal Society of Chemistry. **c**

SEM images of the loaded EGCG fiber are provided, along with the fiber's response mechanism at different pH; Reproduced with permission from ref [93], Copyright 2023, Elsevier. **d** The nanoparticles are discharged from the nanofibers; Reproduced with permission from ref [94], Copyright 2017, American Chemical Society

electrospun with pH-responsive mucoadhesive SPFs [94]. Nanoparticles are released from the SPFs, and peptides are released from the nanoparticles in response to pH changes. Thus, both SPFs and particles are pH-responsive and biocompatible.

4.3 Electrical-Responsive Properties

Materials that respond to electrical stimuli provide direct, noninvasive, and nonpharmaceutical effects on biomolecules and cells and are used in a wide range of biomedical and clinical applications [95]. Many materials can be utilized to create electrical-responsive polymer fibers [96]. Conductive polymers such as polyaniline, polypyrrole (PPy) [97], and PEDOT are considered promising materials that can outperform conventional materials. Low resistivity and voltage are applied to the composite materials of SMPs to facilitate the fabrication of electrically actuated SPFs [98]. The core-shell structures of PLA-PPy fibers

maintained a temperature and sufficient to impart electrical-responsive properties for 2 s at 30 V (Fig. 8a) [99].

Wet-spun phase change material (PCM) microcapsules were embedded in elastic PU to form a dual-response network (Fig. 8b) [7]. In SPFs based on elastic PCMs, organic poly(3, 4-ethylenedioxythiophene): poly(styrene sulfonic acid) bonds the inorganic carbon nanotube/graphene backbone into a 3D hierarchical interconnected sensing network along the elastic fibers, resulting in a high mechanical tensile strength. Thus, this system could adapt to strenuous movements and convert deformation into electrical signals for medical monitoring. By controlling the voltage and pulse time, LM-LCE fibers generated well-controlled deformation in response to electrical stimuli (Fig. 8c) [100]. The internal temperature of the LM interlayer should be higher than that of the LCE enclosure under impulse voltage excitation. Electrical-responsive graphene oxide (GO)/poly(*N*-isopropylacrylamide) (PNIPAM)/sodium alginate hydrogel fibers have a porous

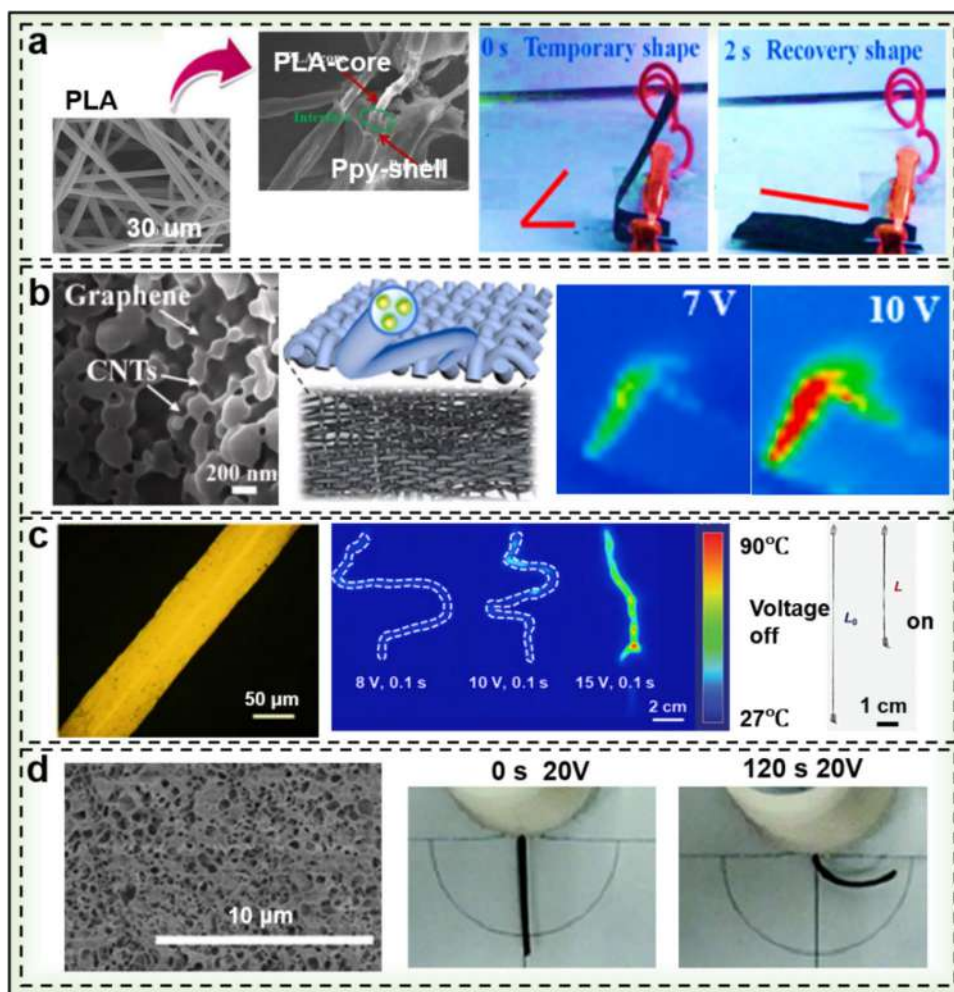


Fig. 8 **a** Shape recovery process of conductive microfiber membrane at 30 V and its SEM image; Reproduced with permission from ref [99], Copyright 2018, American Chemical Society. **b** SEM images of an internal network constructed from carbon nanotubes (CNTs)/graphene connecting micro PCM with different magnifications. The schematic diagram and photograph of plain fabric woven by CNTs-G-PCM@PU fibers. The electrical-responsive diagrams of corresponding infrared images; Reproduced with permission from ref [7], Copyright 2023, Elsevier. **c** The polarized optical micrographs of

LCE fibers. Infrared thermographic images of LM-LCE fibers were stimulated at 8, 10, and 15 V for 0.1 s, respectively. The length of LM-LCE fibers changed before and after 2.4 V 10 s electrical stimulation. Photograph of LM-LCE fibers contracting and lifting a load under electrical stimulation; Reproduced with permission from ref [100], Copyright 2021, John Wiley and Son. **d** GO/PNIPAM/sodium alginate hydrogel fibers and their electrical-responsive properties; Reproduced with permission from ref [101], Copyright 2017, Royal Society of Chemistry

internal structure, displaying bending behavior under noncontact direct current electric fields (Fig. 8d) [101]. They play pivotal roles in numerous applications, including smart sensors, tissue engineering, and drug delivery.

4.4 Light-Responsive Properties

Light-responsive polymer fibers are a class of smart fibrous materials capable of exhibiting specific responses to external light stimuli, such as ultraviolet (UV), visible, or near-infrared radiation (NIR). These fibers are typically fabricated by integrating light-responsive materials (e.g., photochromic molecules, photochromic dyes, or photothermal conversion

materials) into a fiber matrix [76, 102–104]. Their remote precision control, environmental friendliness, and energy efficiency have garnered significant attention.

Cellulose acetate nanofiber composites containing CNTs prepared by ESP exhibit shape memory properties under NIR irradiation (808 nm), and can be used to fabricate soft brakes (Fig. 9a) [105]. The ultrahigh photothermal conversion efficiency of the Fe_3O_4 nanoparticles in the Fe_3O_4 /PAN layer can endow the P(NIPAM-4-benzoylphenyl acrylate) layer with rapid remote-controlled light-responsive deformation (Fig. 9b) [106]. On the basis of the synergistic effect of remote-controlled deformation and remote transportation, this composite hydrogel fiber can be used to design various

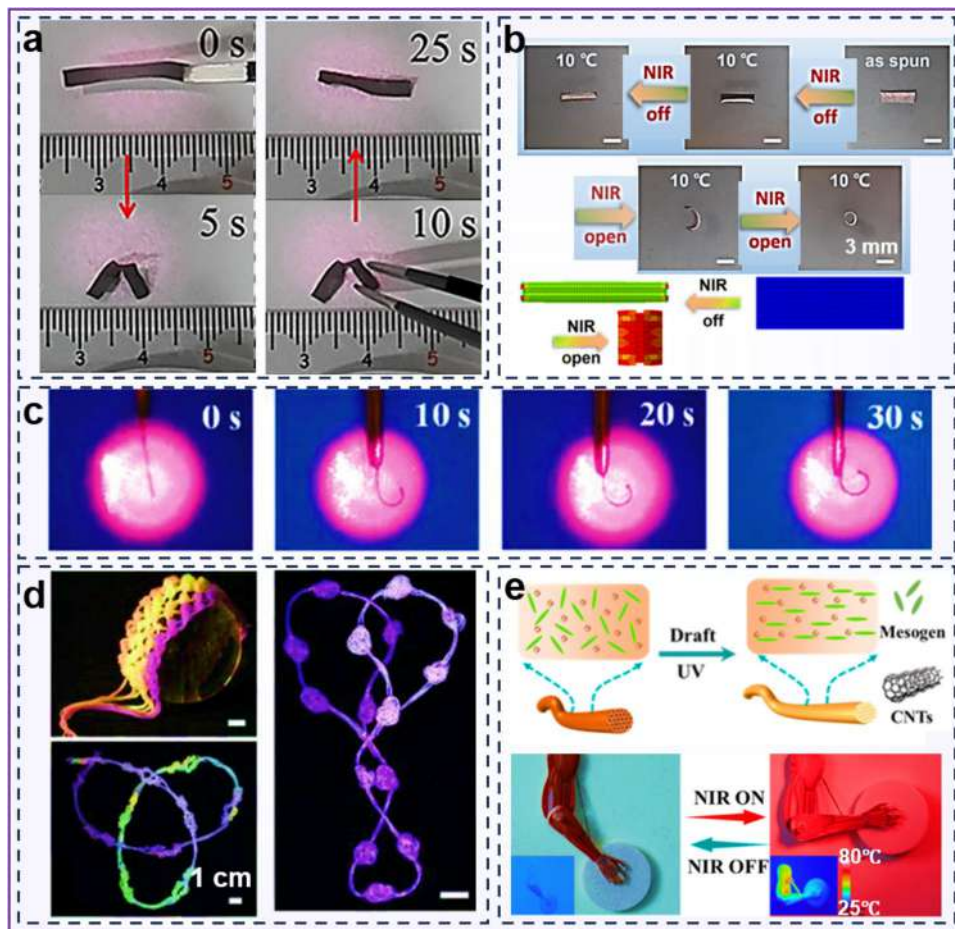


Fig. 9 Macroscopic change diagram of light-responsive properties. **a** NIR-induced shape memory behavior of SMFs; Reproduced with permission from ref [105], Copyright 2023, Elsevier. **b** The bending behavior of the composite hydrogel fiber and its reverse bending under light were analyzed using finite element simulation after the NIR was turned off in cold water; Reproduced with permission from ref [106], Copyright 2021, Elsevier. **c** Shape memory behavior of light-responsive bilayer LHF (living hydrogel

fiber); Reproduced with permission from ref [76], Copyright 2019, John Wiley and Sons. **d** Photograph of living hydrogel fibers with gradient and segmented color change (programmable) taken under visible (left) and UV (right); Reproduced with permission from ref [79], Copyright 2023, John Wiley and Sons. **e** The CNT/LCE composite yarn units within LCE molecules and their yarns mimic artificial muscles; Reproduced with permission from ref [107], Copyright 2024, American Chemical Society

novel biomimetic soft robots. Continuous bilayer hydrogels prepared by microfluidic spinning of linear PNIPAM/calcium alginate/GO semi-interpenetrating hydrogels exhibited bending under NIR irradiation (Fig. 9c) [76]. The functionalization of living hydrogel fibers was achieved using a powerful gene circuit modification method in *E. coli*. Six stained protein genes were introduced into *E. coli* either individually or in combination for cell staining (Fig. 9d) [79]. This modification enables *E. coli* to express colored proteins that cover more than 80% of the color card. Under periodic near-infrared laser irradiation, the CNT/LCE composite yarn contracts, lifting the forearm while the upper arm remains fixed (Fig. 9e) [107]. Owing to their anisotropic, reversible, and programmable shape-changing characteristics, the CNT/LCE composite yarn is highly promising for stimuli-responsive actuators capable of diverse robotic movements.

4.5 Magnetic Field-Responsive Properties

Magnetic field-responsive fibers are a class of fibrous materials that integrate magnetic materials with smart polymer properties. They retain the flexibility, processability, and lightweight characteristics of traditional fibers while exhibiting magnetic field-responsive properties and responsiveness to external stimuli. These fibers are fabricated by combining magnetic nanoparticles (e.g., magnetite [108] and γ -Fe₂O₃), or functional groups with SPFs, enabling functionalities such as shape transformation, cell growth regulation, and drug delivery [109]. The unrestricted nature of magnetic fields allows weak magnetic fields to penetrate non-magnetic and weakly conductive media [110], endowing these fibers with unique advantages in biomedicine, environmental remediation, and smart textiles.

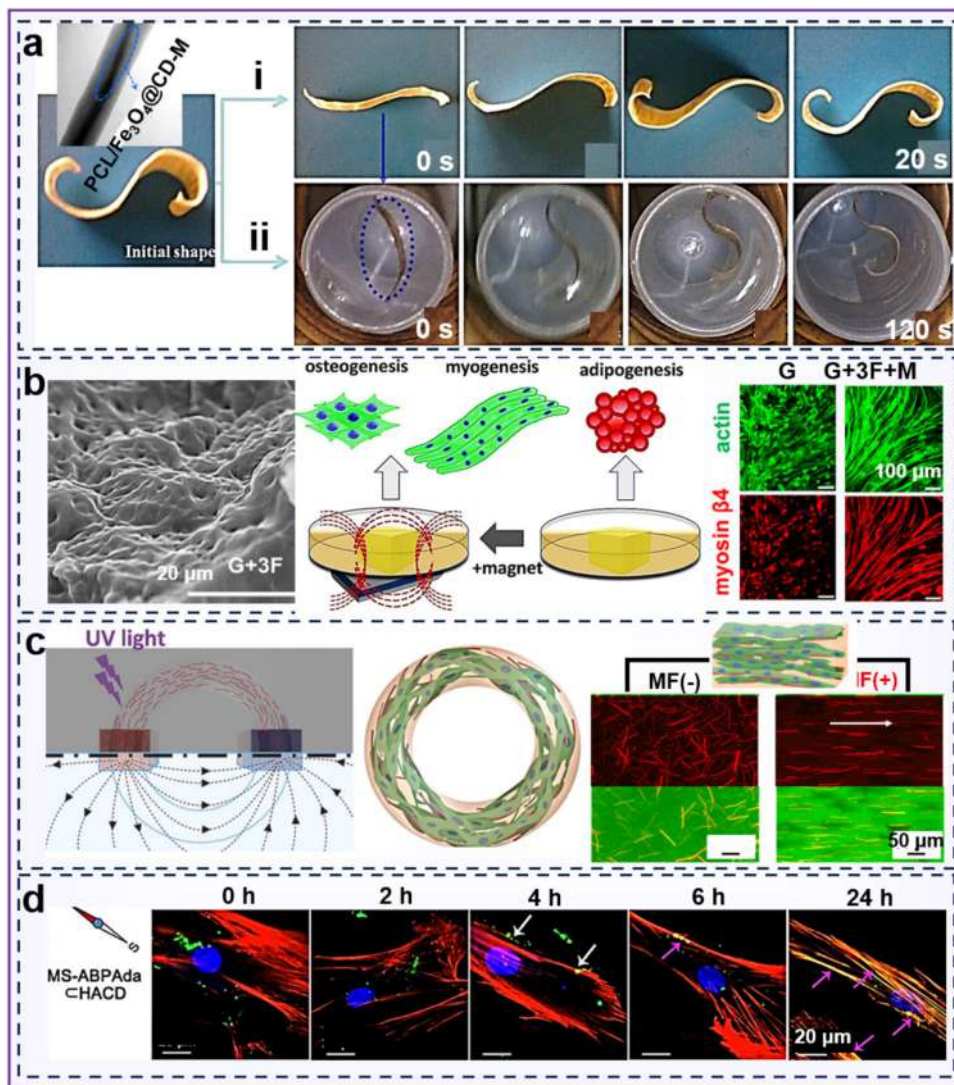


Fig. 10 **a** Transmission electron microscopy (TEM) image of chemically cross-linked PCL/Fe₃O₄@CD-M electrospun composite fibers. A series of photographs depicting the shape memory recovery process of the c-PCL/Fe₃O₄@CD-M composite nanofibers in 46 °C water. (i) and in an alternating magnetic field with a frequency of 20 kHz and a field strength of 6.8 kA m⁻¹. (ii) Reproduced with permission from ref [111], Copyright 2011, Elsevier. **b** SEM micrographs of fragmented nanofibers and (inset) a histogram of the lengths of the fragmented nanofibers. Representative CLSM micrographs of G+3F gel samples. Images of actin and myosin β4-stained C2C12 encapsulated in different composite hydrogel samples over 7 days; Reproduced with permission from ref

[112], Copyright 2023, American Chemical Society. **c** Injectable scaffolds were prepared by encapsulating magnetic field-responsive short nanofibers in GelMa hydrogel. The fluorescence images showed that MSNF60 (red, Nile Red) was encapsulated within GelMa hydrogels (green, FITC); Reproduced with permission from ref [113], Copyright 2022, Elsevier. **d** After 48 h of incubation, the DPSCs were magnetically field-polarized by MS-ABPA da CHACD nanofibers; Reproduced with permission from ref [114], Copyright 2021, American Chemical Society

SPFs were prepared from PCL chemically cross-linked by ESP and CNTs coated with Fe₃O₄ particles as a reinforcing material (Fig. 10a) [111]. SPFs can stimulate Fe₃O₄ nanoparticles in thermal and alternating magnetic fields, and both excitations induce shape recovery. However, permanent shape recovery is faster when triggered by direct heating. Magnetically responsive gelatin fibers were inserted into a gelatin methacryloyl (GelMa) hydrogel for crosslinking to

construct hydrogel fibers (Fig. 10b) [112]. Magnetic Fe₂O₃ particles are enclosed in a small fraction of nanofibers to strengthen the material within physiologically relevant ranges, facilitating the mechanical stimulation of cells encapsulated in 3D.

Injectable remote magnetic nanofiber/hydrogel multiscale scaffolds guided 3D cell alignment and organization by controlling the precise microstructure with a remote magnetic

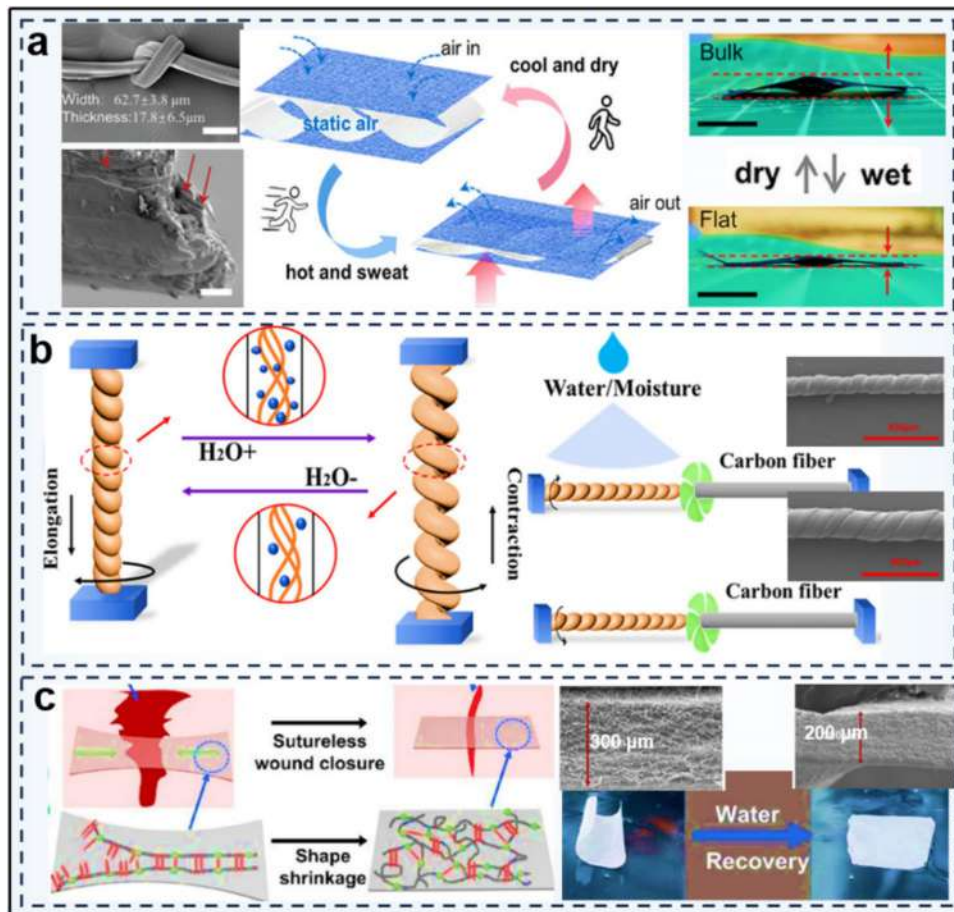


Fig. 11 **a** Knot fiber and its cross-section, where aligned nano-fibrils are indicated by red arrows. Photographs of the programmed state and recovered state of a silk fiber. Illustration of the moisture-actuation stress response mechanism in the regenerated silk fibers. Side view of a prototype of a self-modulated fabric actuated by moisture; Reproduced with permission from ref [119], Copyright 2024, John Wiley and Sons. **b** Illustrates the actuation performance of multi-strand

helical CMC fibers under moisture-responsive properties, showcasing their application in a smart fan powered by moisture; Reproduced with permission from ref [120], Copyright 2023, American Chemical Society. **c** Schematic diagram of self-healing. Moisture-responsive shape recovery process. SEM images of dry and wet PU-fm; Reproduced with permission from ref [117], Copyright 2024, Springer Nature

field (Fig. 10c) [113]. They enabled the replication of native cellular organization by integrating 3D micro- and macro-structures via magnetic field-responsive properties. Biocompatible supramolecular polymer nanofibers were formed by magnetic field-oriented targeting of the actin cytoskeleton using a β -cyclodextrin-grafted hyaluronic acid polymer (HACD) and actin-binding peptide-modified magnetic nanoparticles (MS-ABPAda), which enabled the targeted growth and polarization of stem cells (Fig. 10d) [114].

4.6 Moisture-Responsive Properties

Moisture-responsive polymer fibers are materials that can sense ambient humidity and react accordingly [115]. Internally, these properties manifest in organisms as the precise regulation of the water balance. Externally, they are exemplified by the intelligent adaptation of morphology and structure in response to changes in moisture [116]. The development of moisture-responsive fibers is significant in the field of materials science [48]. In the exploration of biomimetic intelligent materials, researchers have been deeply inspired by the moisture-responsive mechanisms of organisms, successfully developing a series of novel materials that possess

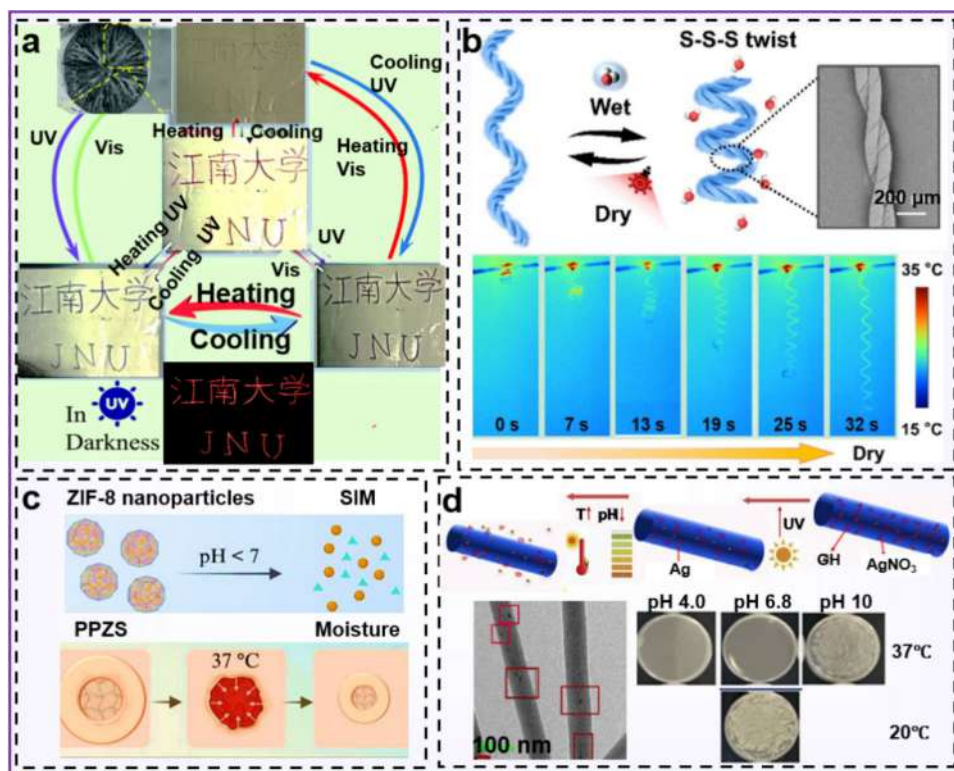


Fig. 12 **a** Fabrication process of the surface of 3% multiple stimuli-responsive fibers. Digital photographs of 7% multiple stimuli-responsive fibers after different stimulations; Reproduced with permission from ref [121], Copyright 2021, Royal Society of Chemistry. **b** Moisture-responsive properties of shell-core fibers with a tertiary spiral structure and infrared images of their elongation; Reproduced with

permission from ref [122], Copyright 2024, Springer Nature. **c** Multiple stimuli-responsive properties of C-PPZS; Reproduced with permission from ref [123], Copyright 2024, Elsevier. **d** PNIPAM NMA-Ac GH+Ag and its antimicrobial effect in response to thermal- and pH-responsive properties; Reproduced with permission from ref [124], Copyright 2021, Elsevier

both moisture-responsive properties and mechanical adaptability [117].

Major ampullate spider silk gland protein 2 (MaSp2) protein contains repeating amino acid sequences that can self-assemble into ordered structures to form strong fibers. When eMaSp2 fibers were exposed to moisture, they shrank by 9.5% when the relative humidity increased from 20 to 90% [118]. The regenerated silk fibers exhibited moisture-responsive and cyclic responses (Fig. 11a) [119]. The shape recovery rate of the silk fibers was approximately 83%, and the maximum actuating stress was 18 MPa, which shows potential for use in moisture-responsive actuators, artificial muscles, and smart textiles. A moisture-responsive actuator consisting of stranded carboxymethyl cellulose (CMC) fibers with a helical structure was prepared using the wet spinning and twisting methods (Fig. 11b) [120]. Owing to its excellent moisture-responsive properties, this actuator was able to untwist while carrying a 5 g load. A moisture-responsive shape memory polyurea-polydopamine-silver film (PU-fm) exhibited excellent toughness, moisture responsiveness, breathability, water absorption capacity

that was four times greater than its weight, and antibacterial properties, all of which contributed to wound closure (Fig. 11c) [117]. PU-fm, equipped with hydrophilic groups, can absorb water molecules, allowing fibers to form hydrogen bonds with water molecules, thereby increasing the degree of slippage between stacked fibers and resulting in greater toughness.

In summary, moisture-responsive fibers exhibit unique properties that allow them to adapt their shape, size, or mechanical behavior in response to changes in environmental humidity. By leveraging these SPFs, researchers can develop innovative applications across various fields, including smart sensors, smart textiles, and environmental monitoring. The development of moisture-responsive fibers holds promise for creating more adaptable, sustainable, and intelligent systems that can interact seamlessly with their surrounding environments.

4.7 Multiple Stimuli-Responsive Properties

The development of modern science and technology has led to increasingly complex performance requirements for smart

Table 1 Materials, structures, stimuli-responsive properties, and applications of SPFs

Material	Structure	Stimuli-responsive property	Application	References
Chitosan/PEO	Random	Temperature	Tissue regeneration	Wei et al. [125]
Epoxy resin/PCL	Porous	Temperature	Drug delivery	Yao et al. [126]
Chitosan/PEO/PCL	Core-shell	pH	Drug delivery	Cheng et al. [127]
PU/EL100-55	Random	pH	Drug delivery	Aguilar et al. [128]
Styrene/butyl acrylate	Random	Light	—	Nezhadghaffar-Borhani et al. [129]
PCL/benzophenone-4-isothiocyanate	Random	Light	Drug delivery,	Chen et al. [130]
PCL/Fe ₃ O ₄	Hollow	Magnetic	Tissue Regeneration	Wang et al. [131]
Poly(succinimide)	Random	Magnetic	Drug delivery, Tissue regeneration	Jedlovsky-Hajdu et al. [132]
PCL/poly(ethylene glycol) /TPU	Aligned	Moisture	Smart sensors	Gu et al. [133]
Silk fibroin	Knot	Moisture	Smart textiles	Xu et al. [119]
PLA/GO	Random	Electricity	Tissue regeneration	Croitoru et al. [134]
PU/GO	Core-sheath	Temperature, Electricity	Color-changing fibers	Zhang et al. [135]
Lignin/PEO	Random	Temperature, Moisture	Biomedicine	Dallmeyer et al. [136]
Pentacosadiynoic acid/PEO	Random	Temperature, Light	Smart sensors	Alam et al. [137]
PAN	Core-shell	Temperature, Electricity	Color-changing fibers	Wang et al. [138]

polymer materials. Fibers that possessed only a single stimuli-responsive property often failed to meet the diverse and complex demands of certain application scenarios. In contrast, fibers with multiple stimuli-responsive properties can respond to a variety of external conditions, greatly expanding their application potential and functionality [85]. SMFs containing PNIPAM-co-acrylic acid (PNIPAM-co-Ac) microgel-loaded PCL nanofibers were demonstrated as SPFs with temperature, pH, and electrical-responsive properties [16]. Refractive measurements at pH values of 4 and 6.5 and in distilled water revealed that the nanofibers responded to temperatures between 31 and 34 °C, as well as to changes in pH, highlighting their suitability for drug delivery.

When multiple stimuli-responsive fibers are heated, their color changes to white because the thermochromic dyes transition to a colorless state at elevated temperatures. Upon exposure to UV irradiation, 7% of the multiple stimuli-responsive fibers turn turquoise. When the temperature is lowered after 5 s of UV irradiation, both thermochromic and photochromic dyes exhibit color changes, resulting in the color of the fibers transforming to a purple hue. Additionally, 7% of the multiple stimuli-responsive fibers emit a bright red color in the dark after UV irradiation (Fig. 12a) [121]. The multiple stimuli-responsive fibers exhibited excellent independent sensitivity to UV and heat, persistent luminescence and stable practical performance. The shell-core spiral fibers were composed of an alginate/poly(ethylene glycol) acrylate shell and an alginate/GO core. Spiral hydrogel fibers exhibit contraction under moisture-responsive property and elongation deformation under light irradiation, which is attributed to the excellent photothermal conversion efficiency of graphene oxide in the core layer and the ultrahigh deformability

of the spiral fibers (Fig. 12b) [122]. As a result, when water evaporates or when the fibers are heated by light, the triple-spiral structure can automatically recover within 32 s.

A poly(trimethylene carbonate) (PTMC)/PVP nanofiber dressing (C-PPZS) with moisture- and thermal-responsive contraction properties was developed for chronic wound healing, featuring pH-responsive drug delivery (Fig. 12c) [123]. The dressing was designed as a four-layer composite structure for convenient storage and exhibited multiple stimuli-responsive properties, including pH-responsive zeolitic imidazolate framework-8 nanoparticles releasing simvastatin and moisture- and thermal-responsive contraction of PTMC/PVP under acidic conditions. Nanoscale silver and gatifloxacin hydrochloride (GH) were incorporated into poly(*N*-isopropyl acrylamide-*N*-methylol acrylamide-acrylic acid) (PNIPAM-NMA-Ac) nanofibers to design pH- and thermal-responsive polymer fiber membranes [124]. At 37 °C/pH 4, PNIPAM-NMA-Ac GH + Ag exhibited more significant antibacterial activity than the platforms containing GH or Ag alone (Fig. 12d).

In conclusion, multiple stimuli-responsive polymer fibers can adapt to complex and changeable environments with diverse functional requirements, thereby providing strong support for innovation and development in many fields.

5 Applications

The excellent stimuli-responsive properties of SPFs lay a solid foundation for their wide applications in numerous fields, including biomedicine [125–127], textiles [119],

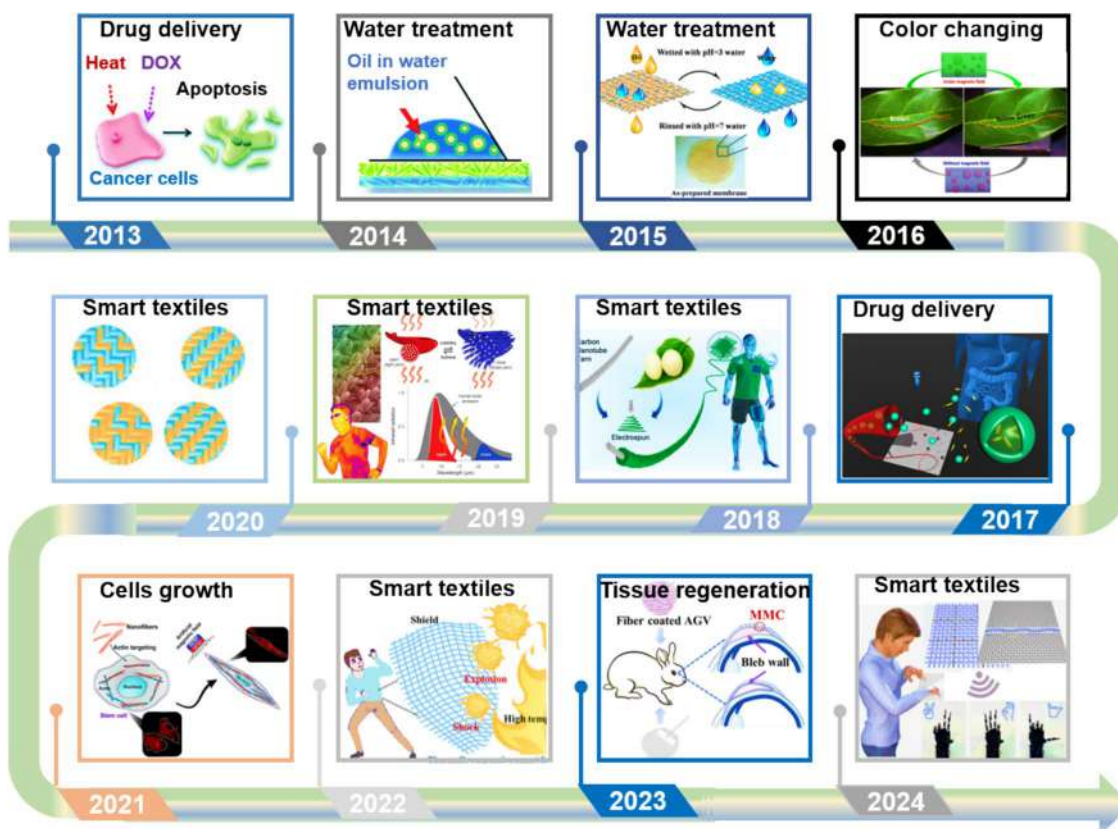


Fig. 13 Smart hyperthermia nanofiber with switchable drug delivery; Reproduced with permission from ref [140], Copyright 2013, John Wiley and Sons. Super wetting nanofibrous membranes for ultrafast oil–water separation; Reproduced with permission from ref [29], Copyright 2014, Royal Society of Chemistry. Membrane for pH-responsive oil/water separation; Reproduced with permission from ref [145], Copyright 2015, American Chemical Society. A new type of photonic crystal PDMS fiber exhibits tunable structural color upon exposure to the external magnetic field; Reproduced with permission from ref [146], Copyright 2016, Elsevier; Reproduced with permission from ref [94], Copyright 2017, American Chemical Society;

Reproduced with permission from ref [147], Copyright 2018, American Chemical Society; Reproduced with permission from ref [148], Copyright 2019, American Association for the Advancement of Science; Reproduced with permission from ref [81], Copyright 2020, John Wiley and Sons; Reproduced with permission from ref [114], Copyright 2021, American Chemical Society; Reproduced with permission from ref [145], Copyright 2022, John Wiley and Sons; Reproduced with permission from ref [23], Copyright 2023, Springer Nature; Reproduced with permission from ref [149], Copyright 2024, Springer Nature

sensors [133], the environment, color-changing fiber [135, 138], automotive, and construction sectors (Table 1) [139].

SPFs can respond to various environmental changes, demonstrating remarkable advancements across multiple technical areas from 2013 to 2024 (Fig. 13). SPFs have proven beneficial in drug delivery [23, 140, 141] by promoting cell growth in cancer treatment, specifically by releasing DOX to trigger cancer cell apoptosis [140]. They also show great promise in water treatment with excellent oil–water separation ability [29] and water adsorption capacity [142]. SPFs have been utilized as color-changing fibers because they change color in response to environmental variations [28]. Moreover, in the realm of smart textiles [143], SPFs are capable of being fixed into a specific spiral shape at high temperatures and restoring their original shape after

the removal of external forces and thermal sources, thereby effectively regulating heat [144]. Additionally, SPFs are responsive to thermal stimuli, enabling signal transmission that varies accordingly, which facilitates the preparation of smart sensors [27]. By carefully designing and manipulating the microstructures of aligned fibers in combination with magnetic particles, cell growth and axon elongation can be induced under the action of a magnetic field, thereby promoting tissue regeneration [113].

5.1 Cell Growth

Traditional biomimetic scaffolds are mostly static structures, which cannot accurately reproduce the complex dynamic microenvironments of living organisms, thereby limiting

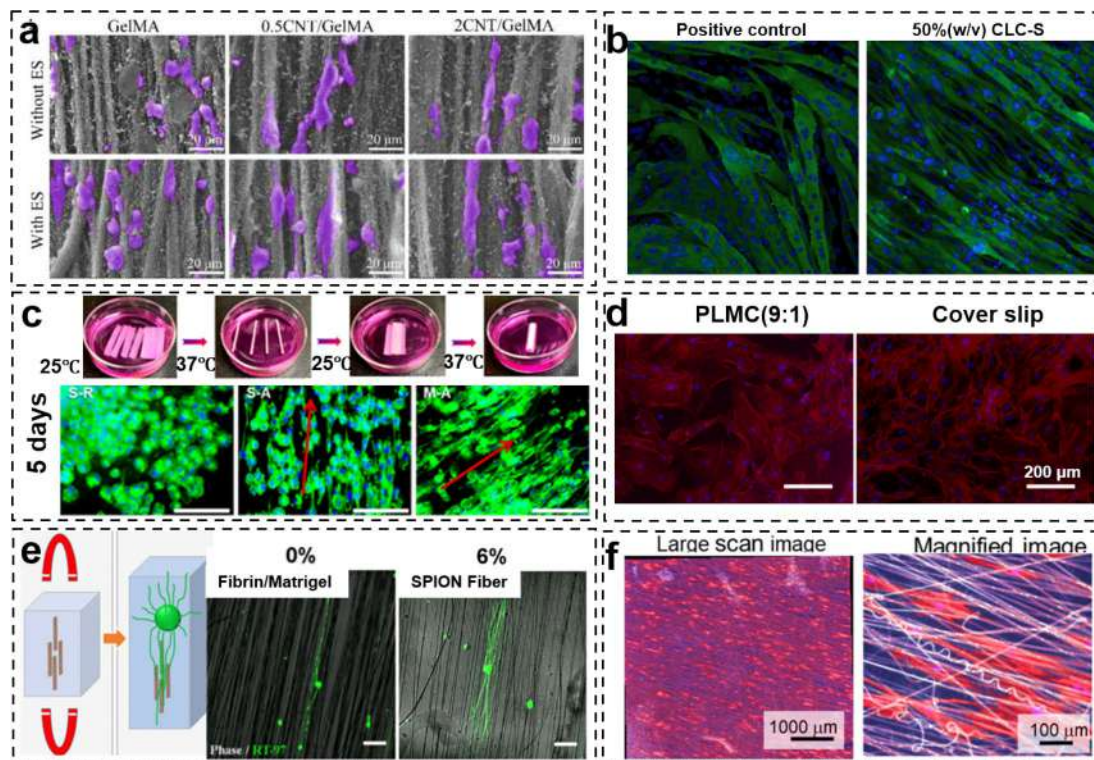


Fig. 14 **a** Laser confocal images of PC12 cell adhesion and neural stem cells cultured on hydrogel fibers with and without electrical excitation; Reproduced with permission from ref [154], Copyright 2024, Elsevier. **b** Immunohistochemistry staining of myosin heavy chain and 4', 6-diamidino-2-phenylindole of C2C12 mouse myoblast cells cultured on 50% (w/v) CLC-S compared to positive control; Reproduced with permission from ref [24], Copyright 2020, American Chemical Society. **c** Immunofluorescence map of Schwann cell growth on a shape memory PLATMC multiple channel nerve guidance conduit; Reproduced with permission from ref [26], Copyright

2020, American Chemical Society. **d** Immunofluorescence map of cell growth on PLMC; Reproduced with permission from ref [89], Copyright 2014, American Chemical Society. **e** The superparamagnetic Fe_2O_3 nanoparticles combined with PLLA fibers in a hydrogel promote axon elongation; Reproduced with permission from ref [31], Copyright 2019, American Chemical Society. **f** Adhesion morphology and arrangement of human mesenchymal stem cells on stretched PCL-based PU nanofibers; Reproduced with permission from ref [155], Copyright 2019, Molecular Diversity Preservation International

their applications in bioengineering [150]. By culturing cells on SPFs scaffolds, their morphology can be adjusted to mimic the dynamic environment within the native organism more effectively for enhancing the biocompatibility and functionality of biomimetic materials [151].

The development of a novel cell-adhesion peptide-functionalized thermal-responsive polymer fiber scaffold was demonstrated based on PLA and poly(2-(2-methoxyethoxy) ethyl methacrylate) for enzyme-free 3D mammalian cell culture [152]. The photothermal electrospun nanofibers were fabricated by incorporating light-responsive iron oxide nanoparticles within biocompatible SPFs [153]. These nanofibers promoted membrane permeability in a variety of cell types without exposure to potentially toxic photothermal nanoparticles, paving the way for the safe and efficient production of engineered cells for therapeutic application and clinical translation.

As shown in Fig. 14a, CNT/GelMa hydrogel fibers mimic the arrangement, conductivity, and soft mechanical

properties of nerve axons [154]. Axon-like hydrogel fibers support the viability and aligned adhesion of rat adrenal medulla pheochromocytoma (PC12) cells, and their performance is enhanced by electrical-responsive properties. Electroexcitation binds to the arranged CNTs/GelMa fibers to promote the neuron-directed migration and differentiation of neural stem cells. A nonwoven cholesteryl ester liquid crystal scaffold (CLC-S) was prepared using ESP by mixing cholesterol oleoyl carbonate, cholesterol nonanoate, and benzoate cholesterol lipids in PCL (Fig. 14b) [24]. By adjusting the component ratios, LC material with an intermediate phase temperature of 36–40 °C was obtained, which matched the temperature range used for cell culture. The incorporation of the scaffold as a biomimetic interface enhanced cell adhesion and proliferation and promoted the formation of myofibrils in mouse myoblasts cultured in vitro.

Shape memory poly(lactide-co-trimethylene carbonate) (PLATMC) nanofibers were used to fabricate a multichannel nerve guidance conduit (Fig. 14c) [26]. After being

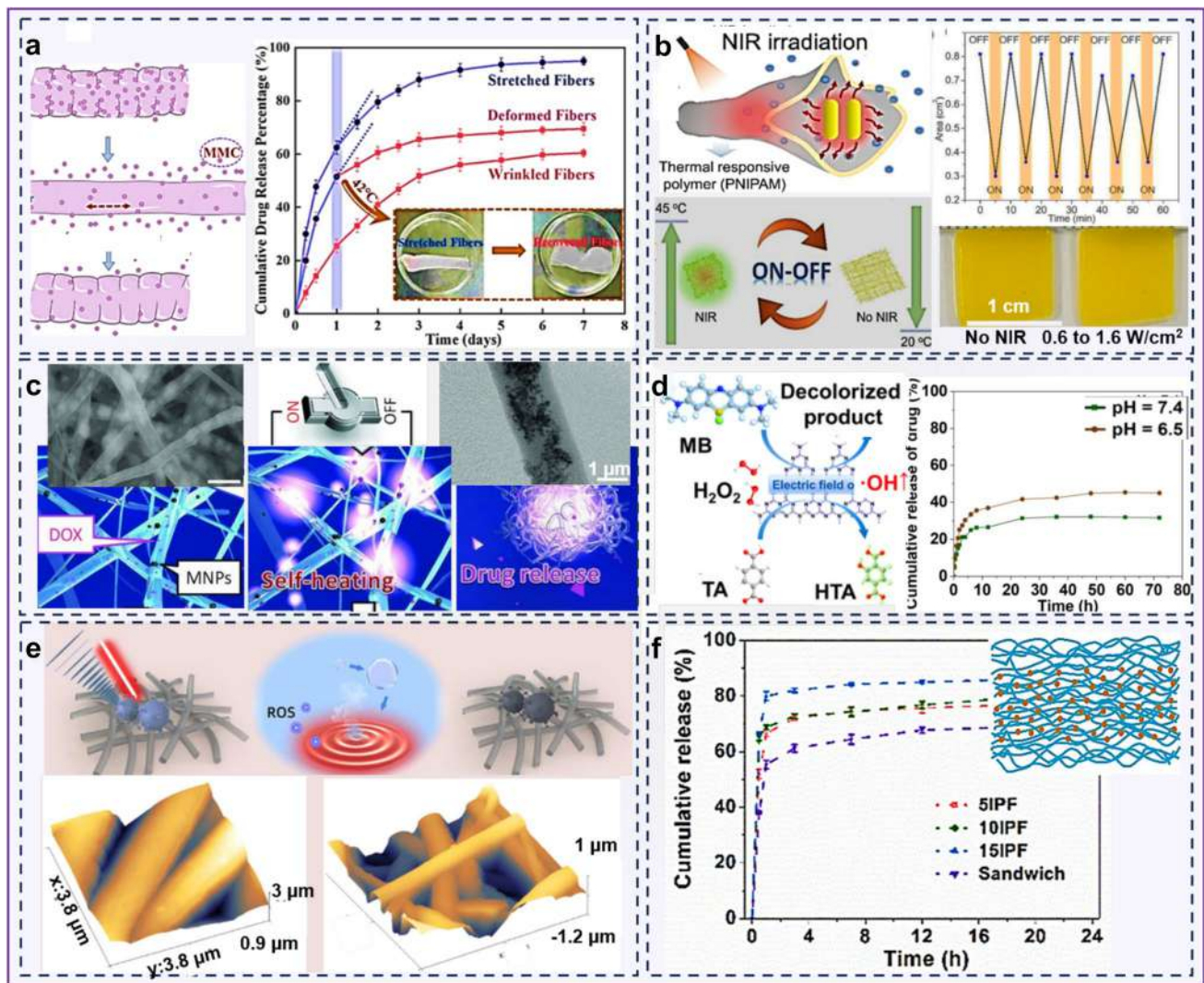


Fig. 15 **a** Application of shape memory PLA/PPDO fiber membranes in drug delivery; Reproduced with permission from ref [23], Copyright 2023, Springer Nature. **b** Schematic illustration showing the thermal-responsive release of fluorescein from nanofibers containing gold nanorods upon NIR irradiation. Function relationship of temperature change area change of PNIIPAM fiber under light-responsive properties; Reproduced with permission from ref [166], Copyright 2021, Multidisciplinary Digital Publishing Institute. **c** Schematic illustration showing the thermal-responsive release of DOX and the cumulatively released percentages of DOX with alternating cycles of “ON–OFF” switching; Reproduced with permission from ref [140], Copyright 2013, John Wiley and Sons. **d** Catalytic and drug release

properties of the gelatin/PCL nanofibrous patch integrates DOX and graphitic carbon nitride; Reproduced with permission from ref [169], Copyright 2023, American Chemical Society. **e** Schematic illustration and atomic force microscope images of PCL/gelatin electrostatic scaffold and coating with chlorin e6@pCN and GO and synergistic sonophotodynamic therapy for breast cancer via 808 nm laser and 1 MHz ultrasound; Reproduced with permission from ref [170], Copyright 2020, American Chemical Society. **f** Schematic diagram illustrating the fabrication of the sandwiched poly(lactic-co-glycolic acid) (PLGA)/PCL scaffold and cumulative release of ibuprofen; Reproduced with permission from ref [25], Copyright 2020, Elsevier

seeded with Schwann cells and incubated for 7 days, the cells on the multichannel catheter exhibited enhanced proliferation, which was attributed to the numerous adhesion sites that provided a favorable microenvironment for axon extension. Furthermore, biodegradable PLMC nanofibers are cytocompatible as they support cell adhesion and proliferation and promote biomineralization-associated alkaline phosphatase expression and mineral deposition

(Fig. 14d) [89]. A magnetic electrospun PLLA fiber scaffold can be manipulated through in situ injection of hydrogel combined with an external magnetic field, where the hydrogel provides guidance for cell growth, thereby promoting the alignment and length of neurites within the nerve guidance conduit (Fig. 14e) [31]. The mechanical properties of a basal culture substrate affected the attachment of human mesenchymal stem cells to PCL-based PU

nanofibers via integrin and focal adhesion kinase signaling, resulting in the reorganization of the actin cytoskeleton in response to external mechanical signals, thereby promoting cell orientation and growth (Fig. 14f) [155].

5.2 Drug Delivery

An ideal drug delivery system is crucial for enhancing therapeutic efficiency and reducing the toxicity and side effects of drugs [156]. Nanofiber membranes offer considerable potential in the application of wound dressings and controlled drug delivery owing to the controllable “on–off” switching of SPFs in response to stimuli and their very thin films and high drug-loading capacity [157]. Drug delivery systems regulate the distribution of their drugs in living organisms in terms of time, space, and dose [158, 159]. Owing to their characteristics of lesion targeting, great drug encapsulation efficiency, and compatibility with a variety of drugs, SPFs are widely used in drug delivery and hold great promise for applications in the biomedical field.

Core–shell SPFs are composed of two different materials: the drug is in the inner core, while the shell provides additional protection against premature release or release in unsuitable environments [160]. Thermal-responsive drug-loaded SPFs were prepared using ESP combined with UV photopolymerized PNIPAM as the shell and biodegradable PLA as the core. Combretastatin A4 was loaded in the PLA, and thermal-responsive core–shell nanofibers controlled the drug release rate under heating by surface plasmon resonance [161]. The thermal-responsive PNIPAM nuclear layer expands and contracts to achieve programmable drug release from core–shell nanofiber scaffolds [162]. The anticancer drug doxorubicin hydrochloride (DOX) was encapsulated in cross-linked PNIPAM/gelatin nanofibers. When the temperature increases above the critical dissolution temperature, a thermal-responsive drug is released on demand, thereby reducing the viability of HeLa cells [163]. Thermal-responsive composite SMPU fibers prepared with a core–sheath structure achieved the sustained release of berberine chloride hydrate over an extended-release period [164].

The functional layered structure of two-component composite fiber membranes enables the spatiotemporal control and graded release of drugs through in situ cross-linking, which can effectively promote wound healing. This system takes advantage of the differences in drug release rates between internal and superficial fibers with different structures to achieve a synergistic effect between the two drugs [165]. The macroscopic stretching and shape memory effects of PPDO/PLA fibers can convert the fiber surface morphology between folds and smooth morphologies, which is favorable for drug delivery (Fig. 15a) [23]. PNIPAM composite nanofibers loaded with GNRs enable controlled drug

release via NIR irradiation (Fig. 15b) [166]. The temperature produced by the GNRs guaranteed the contraction of the PNIPAM nanofibers to facilitate the drug release, which was controlled by the NIR power density to provide on-demand drug delivery.

Novel thermal- and pH-responsive PNIPAM-NMA-Ac microfibers were developed via radical copolymerization, ESP, and thermochemical treatments, which were demonstrated for smart sensors and drug delivery [167]. SMPU/hydroxyapatite biomimetic composites were prepared and loaded with dexamethasone as a model drug [167]. Hydroxyapatite enhanced the degradation rate of the SMPU fibers, ensuring sustained drug delivery. Furthermore, electrospun copolymers of *N*-isopropylacrylamide and *N*-hydroxymethylacrylamid nanofibers containing DOX and magnetic nanoparticles were prepared with switchable drug release to induce cancer apoptosis (Fig. 15c) [140]. Figure 15d shows that the peroxidase-like activity of graphitic carbon nitride in the nanofibrous patch, which generates hydroxyl radicals ($\bullet\text{OH}$), can be enhanced by 4.12 times through its electrical-responsive properties. Simultaneously, DOX can be released to synergize with the treatment in the weakly acidic tumor microenvironment [169]. Chlorin e6-loaded PCL/gelatin light-responsive scaffolds with GO exhibit increased surface roughness and enhanced sonodynamic and photodynamic activities for efficient breast cancer treatment (Fig. 15e) [170].

The sandwich model refers to a system in which a drug is placed between two layers of material to form a sandwich-like structure. This structure can provide a more uniform drug distribution, and the rate of drug delivery can be controlled by adjusting the material of the middle layer. Figure 15f shows the selection of ibuprofen as the drug model, with PLGA and PCL being used as fibrous membrane materials. A new sandwich structure was constructed with an ibuprofen fibrous membrane to reduce sudden release and achieve a prolonged release of the drug, thereby improving its antiadhesion effect and anti-inflammatory properties [25].

SPFs have revolutionized drug delivery systems by offering precise spatiotemporal control, high drug-loading capacity, and stimuli-responsive release mechanisms. These fibers enable on-demand drug release through external stimuli such as thermal, pH, moisture, or light. Additionally, functional layered structures and sandwich models allow for graded drug release and synergistic therapeutic effects, making them highly effective in wound healing and cancer treatment. However, challenges remain, including the complexity of fabrication, potential biocompatibility issues, and the need for further optimization of release kinetics. Future advancements could focus on integrating multi-stimuli responsiveness, improving biodegradability, and expanding applications in personalized medicine and regenerative therapies.

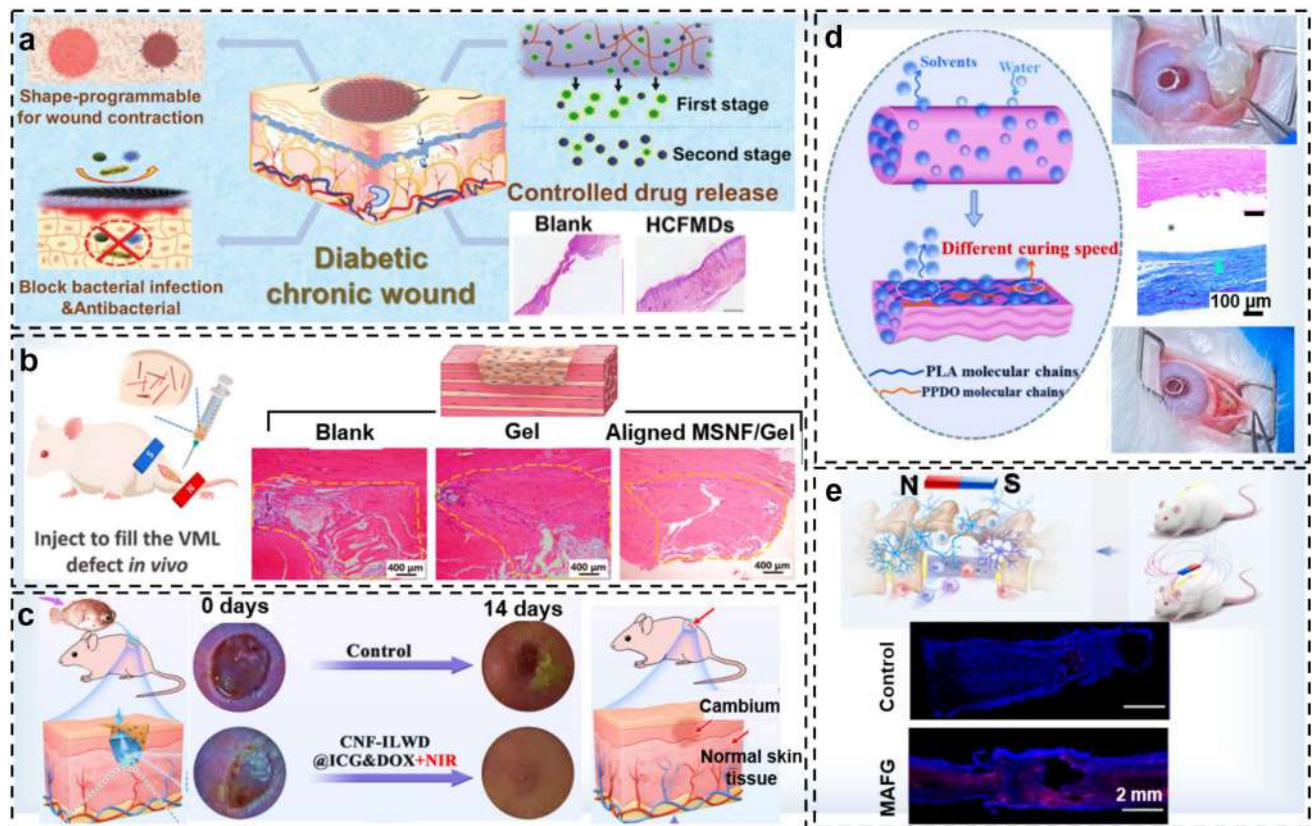


Fig. 16 **a** Schematic diagram of the skin wound healing process and its H&E staining in diabetic mice under different treatments; Reproduced with permission from ref [165], Copyright 2022, John Wiley and Sons. **b** The ultrasound images show that a rat VML model was repaired with an aligned MSNF/Gel scaffold 2 weeks later. The yellow box indicates the defective area; Reproduced with permission from ref [113], Copyright 2022, Elsevier. **c** Photographs were taken of staphylococcus aureus infection wounds at 0 and 14 days in the

control group and CNF-ILWD@ICG+NIR group; Reproduced with permission from ref [174], Copyright 2021, American Chemical Society. **d** Anti-scarring effect of PLA/PPDO fiber membranes; Reproduced with permission from ref [23], Copyright 2023, Springer Nature. **e** Magnetic field-responsive properties of BDA in the control and MAFG groups; Reproduced with permission from ref [175], Copyright 2024, Elsevier

5.3 Tissue Regeneration

In tissue engineering, the design of bio-scaffolds prepared with SPFs as key elements to support and guide cell growth must closely mimic the natural structure and chemical composition of the extracellular matrix [171]. Owing to their unique 3D network morphology, SPFs promote the efficient migration and firm adhesion of cells and accelerate cell growth, providing an ideal microenvironment for tissue regeneration [172]. In addition, the pores between the fibers are carefully designed to ensure efficient nutrient delivery and promote neovascularization, which is essential for tissue repair [173].

Figure 16a shows a thermal-responsive PLATMC crosslinked GelMa/PAA composite fibrous membrane. The membrane contains metformin and simvastatin and has temperature-responsivity, bacteriostatic and hydrophobic effects, as well as a programmable shape [165]. This membrane promoted chronic wound healing in diabetic patients

in vivo, with significantly higher healing rates than those of the dexamethasone acetate film and blank treatment groups. The management of volumetric muscle loss (VML) injuries caused by severe trauma or tumor ablation is a clinical challenge because muscle loss exceeds the self-healing capacity [113]. Linearly stacked peri-muscular areas were observed after 2 weeks of treatment with the aligned MSNF/gel and gel groups (Fig. 16b). In contrast, fibrous scar tissue was present in the blank group, suggesting that the injectable MSNF/gel scaffold contributed to the functional recovery of VML [113]. As shown in Fig. 16c, cellulose nanofiber (CNF) wound dressings use NIR light to trigger a multimodal treatment mechanism through synergistic photothermal, photodynamic, and chemotherapy effects, providing highly effective treatment of drug-resistant bacterial infections and tumor cells [174]. Scarring in the filtering bleb after glaucoma drainage device implantation was mitigated by the PLA/PPDO fiber membrane, which extended the range of biomedical applications for SMP fibers (Fig. 16d)

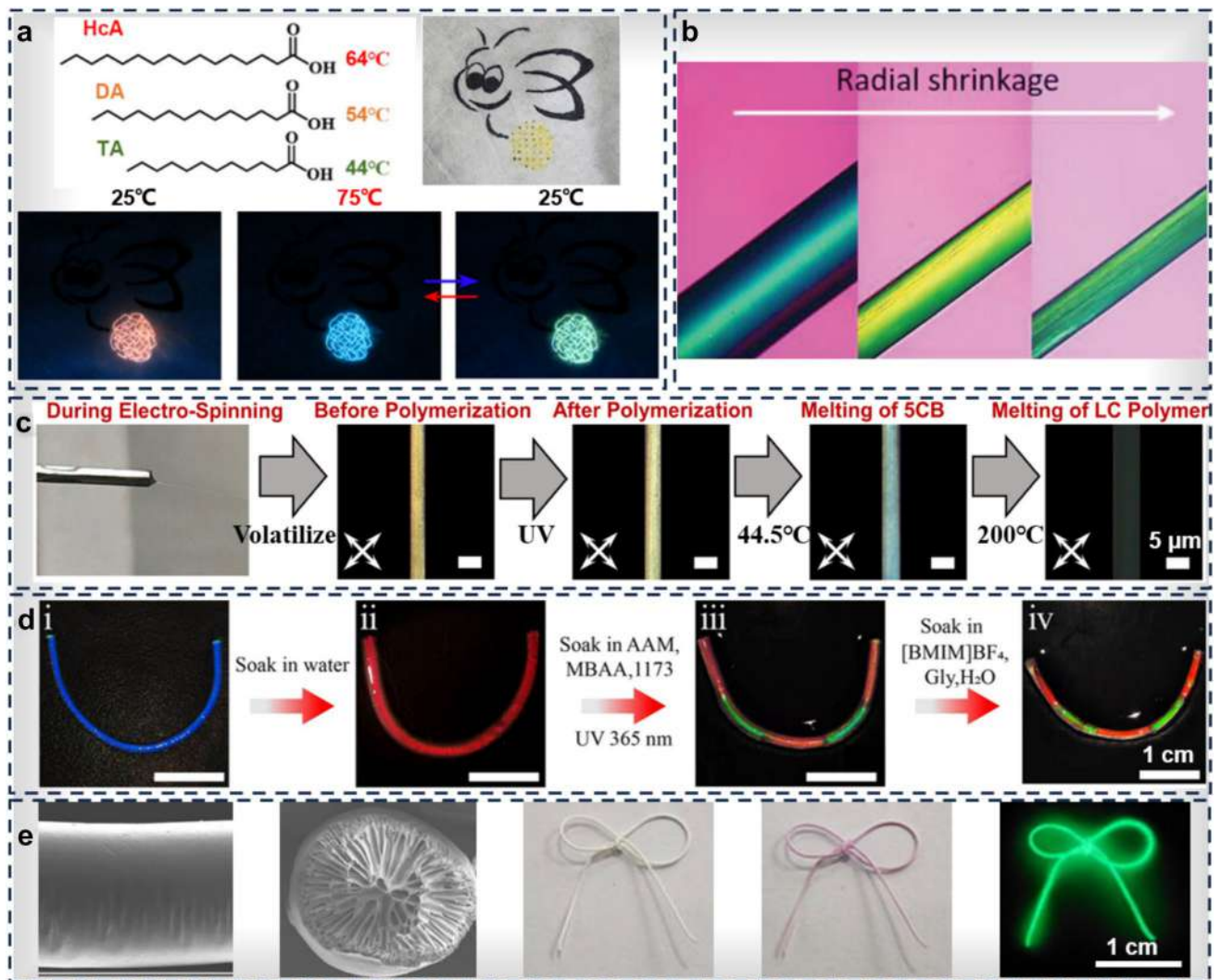


Fig. 17 **a** Photos of the coumarin/HcA composite fibers exhibiting thermal-responsive tunable fluorescence; Reproduced with permission from ref [28], Copyright 2021, American Chemical Society. **b** The transmitted color change of the LMC fibers from cyan to yellow to green upon the loss of water loss; Reproduced with permission from ref [81], Copyright 2020, John Wiley and Sons. **c** The effect of UV exposure on the phase transition temperature of liquid crystal core-sheath fiber within a coaxial electrospun polymer net-

work; Reproduced with permission from ref [32], Copyright 2023, American Chemical Society. **d** Digital photographs of hydrogel fibers at various stages of the compilation process; Reproduced with permission from ref [46], Copyright 2022, American Chemical Society. **e** Multiple stimuli-responsive polymer fibers and their fast-response reversible photochromic and luminescent properties; Reproduced with permission from ref [180], Copyright 2020, Elsevier

[23]. Figure 15e shows a magnetic field-responsive aligned nanofiber hydrogel (MAFG) that combines the structural orientation of nanofibers and the flexibility of the fibrin hydrogel [175]. The changes in magnetic field-responsive polymer fibers result in a significant alignment of neurons and recruitment of endogenous neural stem cells, ultimately promoting their differentiation into neurons.

PLMC composite nanofiber scaffolds containing hydroxyapatite can effectively promote the formation of osteoblasts after 14 days of cell culture in vitro, showing

their potential as bioactive scaffold materials in bone tissue engineering. The preferential hydrolysis of GA groups within the block copolymers of degradable magnesium/PLGA composite fiber membranes, which is catalyzed by alkalis, along with changes in their microstructure, serves to enhance cell adhesion and activates angiogenesis. In addition, enhanced tissue infiltration and revascularization in refractory rabbit urethral wounds, along with accelerated tissue repair and functional recovery, were observed. Owing to their excellent biocompatibility and functionality, SPFs

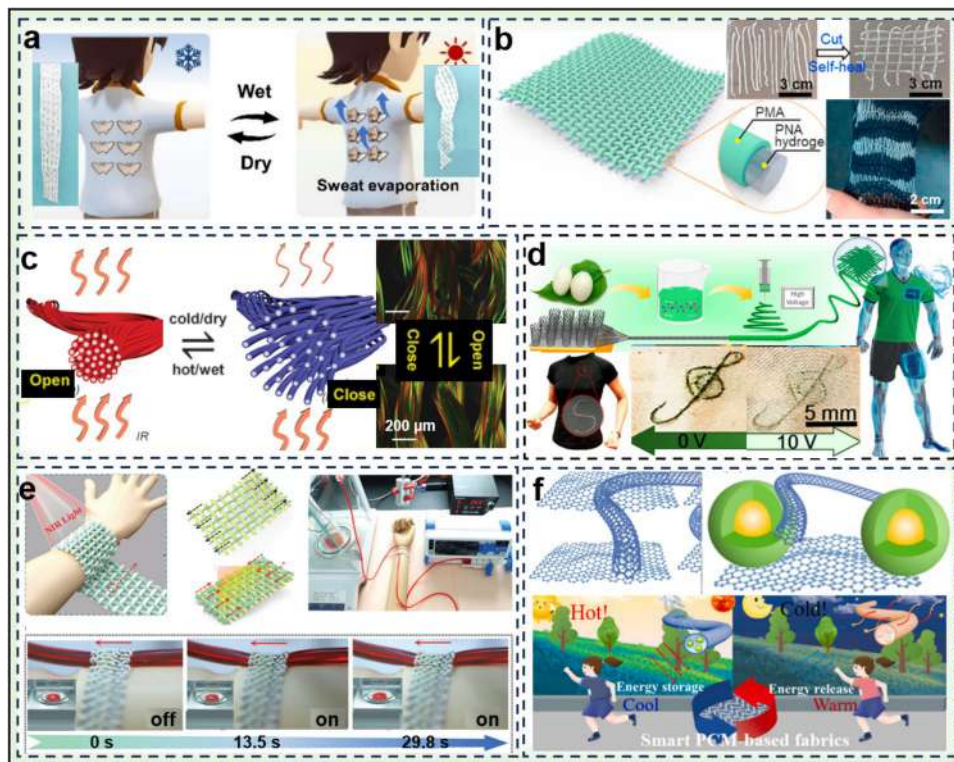


Fig. 18 **a** Under dry conditions or light irradiation, the structure of the core-shell fibers undergo contraction and reverts to its initial spiral state by expelling water. Smart textiles designed for thermal management exhibit distinct performance under dry and wet skin conditions; Reproduced with permission from ref [122], Copyright 2024, Springer Nature. **b** Schematic diagram of a TNG textile woven from PNA/PMA core-sheath fibers with a reversible solgel transition of PNA and its hydrogel fibers self-healing into a network structure after cleavage; Reproduced with permission from ref [183], Copyright 2020, Elsevier. **c** Dynamic changes of microscopic and macroscopic patterns and moisture-responsive smart textile microfibers in response to light-responsive properties; Reproduced with permission from ref

[148], Copyright 2019, American Association for the Advancement of Science. **d** Fabrication and application of CNT@silkwire; Reproduced with permission from ref [147], Copyright 2018, American Chemical Society. **e** Schematic diagram and reversible deformation mechanism of a light-responsive hemostatic bandage that slows down the physical image of fluid flow on the simulated arm; physical image of tightening the infusion tube; Reproduced with permission from ref [184], Copyright 2024, John Wiley and Sons. **f** The schematic of temperature regulation illustrating the thermal storage and release processes in smart textiles based on CNTs-G-PCM@PU; Reproduced with permission from ref [7], Copyright 2023, Elsevier

scaffolds show great promise for advanced medical applications requiring complex structures and functionalization.

SPFs, particularly those designed as bio-scaffolds, play a pivotal role in tissue engineering by closely mimicking the natural extracellular matrix and providing a network structure that supports cell migration, adhesion, and growth. These fibers, with their programmable shapes, controlled drug-release capabilities, and stimuli-responsive properties, are highly effective in promoting wound healing, muscle regeneration, and bone formation. Additionally, their precisely designed porous structures ensure efficient nutrient delivery and neovascularization, which are critical for tissue repair. However, challenges remain, including issues related to biocompatibility, long-term safety, and the need for further optimization of mechanical properties and degradation rates. Future advancements could focus on developing SPFs with multi-stimuli responsiveness and enhanced

biodegradability, enabling their application in complex tissue regeneration and customized smart medicine.

5.4 Color-Changing Fibers

Color-changing fiber is a category of fiber with a specific composition or structure that automatically alters its color when stimulated by environmental factors such as thermal [176], moisture, electricity, or light [177, 178]. These fibers have been demonstrated to be applicable in personal thermal management [178], smart displays, and radiant cooling windows [179].

Multiple color-reversible electrochromic silver nanoparticles/reduced graphene/PU conductive fibers exhibited excellent electrothermal and color-changing properties [135]. Coumarin/hexadecenoic acid (HcA) microemulsion particles were introduced into an alginate fiber matrix, enabling rapid

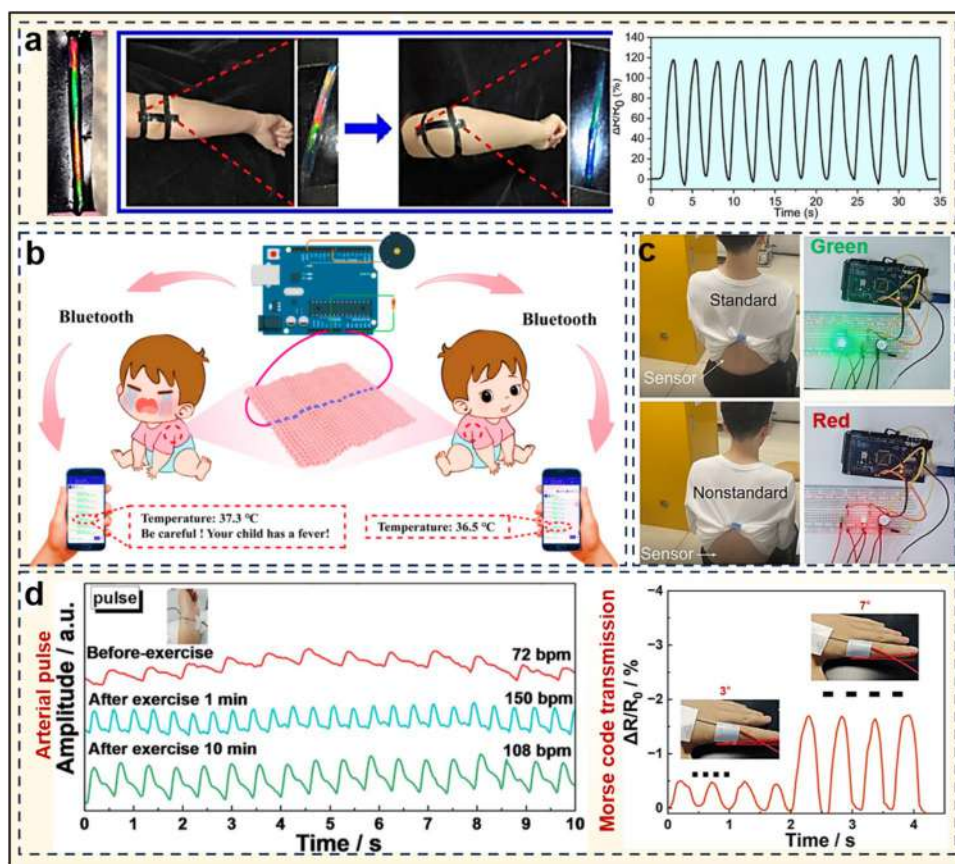


Fig. 19 **a** Heterogeneous interactive smart sensor monitors changes in the electrical signal and the corresponding photographs when the human elbow is bent; Reproduced with permission from ref [46], Copyright 2022, American Chemical Society. **b** Application of PU/graphene@PEDOT:PSS smart textiles for monitor children's body temperature; Reproduced with permission from ref [34], Copyright 2023,

American Chemical Society. **c** The CHF-5 sensor monitors sitting posture; Reproduced with permission from ref [190], Copyright 2021, American Chemical Society. **d** The hydrogel fiber sensor monitors pulse before and after exercise and transmits Morse code; Reproduced with permission from ref [47], Copyright 2024, American Chemical Society

and reversible switching of thermochromic fluorescence under 365 nm UV light (Fig. 17a) [28]. Hierarchical LMC fibers with a core-sheath structure was fabricated using cellulose nanocrystals within a hydrogel sheath formed in situ (Fig. 17b) [199]. Because of their unique topological architecture, the LMC fibers can be controlled by the direction and intensity of polarized light and act as stimuli-responsive materials for chiral optical sensing, polarization-based encryption, and smart textiles.

A homogeneous medium of polymer LC core-sheath fibers prepared by ESP exhibited yellow interference (Fig. 17c) [32]. The orientation of the medium was stabilized by UV crosslinking, but as the temperature increased, the interference color gradually changed to blue, indicating that the arrangement of the medium was disturbed. As shown in Fig. 17d, homogeneously colored single-network hydrogel fibers were prepared by injecting hydrogel precursors into microtubules and co-assembling them with dodecyl itaconic acid glycerides and monomeric AAM,

followed by polymerization under UV irradiation [46]. Subsequently, by immersion and selective light treatment, bicolor heterogeneous hydrogel fibers with alternating single and double networks were formed, which exhibited redshifted colors corresponding to lattice spacing changes. Photochromic pigments, $\text{SrAl}_2\text{O}_4: \text{Eu}^{2+}, \text{Dy}^{3+}$ phosphors, and photochromic pigments were doped into PAN fibers, which exhibited fast responsivity and reversible photochromic properties under a wide range of excitation wavelengths (300–450 nm), with a maximum broadband peak at 525 nm (Fig. 17e) [180].

5.5 Smart Textiles

Smart textiles not only retain the flexibility, comfort, and wearability of traditional textiles but also endow them with intelligence, interactivity, and multifunctionality [180]. They represent a product of interdisciplinary integration among textile science, materials science, electronic engineering,

and biomedical engineering. Owing to their lightweight nature, flexibility, high porosity, and multiple integrated functionalities, smart textiles hold immense promise for personal thermal management [181, 182].

Spiral hydrogel fibers, which form a tightly interwoven structure with polyester yarns, experience uneven external stress due to rotational deformation upon wetting, causing the smart textiles to exhibit curling deformation (Fig. 18a) [122]. Owing to the excellent moisture and photothermal response efficiency of the fibers, their application in smart textiles enables highly efficient thermal management of the human epidermis. As shown in Fig. 18b, a PNA core was coated with poly(methyl acrylate) (PMA) to produce core-sheath fibers with strain-sensing functionality suitable for monitoring human movement [183]. In addition, triboelectric nanogenerator textiles woven from PNA/PMA fibers are manufactured to convert mechanical energy into electrical energy.

As shown in Fig. 18c, the relative change in the infrared transmittance exceeds 35% when the relative humidity changes in the smart textiles [148]. A silk nanofiber and wound CNT yarn were used to form a CNT@silk wire, which was used to fabricate electrochromic patterns and flexible near-field communication coils, exhibiting its potential as circuits or wires in smart fabric electronics (Fig. 18d) [147]. Novel gold nanorods (AuNRs) with a bionic spider web structure exhibited super-shrinkage deformation in an LCE yarn actuator (Fig. 18e) [184]. The photopolymerizable AuNRs were uniformly crosslinked within an LCE molecular chain, and the smart yarn exhibited stable long-term light absorption and photothermal super-deformation performance. Light-responsive microswimmers based on AuNR@LCE yarn moved quickly on water surfaces, while smart hemostatic bandages made from the same material effectively achieved hemostasis under light-responsive properties.

The highly elastic CNTs-G-PCM@PU fibers not only exhibit excellent responsiveness to multiple stimuli such as electricity, temperature, and light but also convert energy into latent heat, enabling personalized thermal management during the response process (Fig. 18f) [7]. Furthermore, these stimulus-responsive SPFs, with mechanical stretchability exceeding 200%, can seamlessly adapt to the curved surfaces of human skin and transform mechanical deformations into characteristic signals for personalized health monitoring. Stretchable conductive PCM-based SPFs exhibit excellent Joule heating and photothermal effects and can convert multiple excitations into latent heat energy that is stored for self-powered personal thermal management. Furthermore, PCM-based SPFs have excellent knotting ability and can be woven into large, breathable textiles.

5.6 Smart Sensors

Smart sensors, as implantable devices, play crucial roles in health monitoring, disease prevention, and control [185]. These sensors are widely utilized in biomedical fields for real-time monitoring of various physiological indicators, such as motion, pulse, sitting posture, and body temperature. They offer significant advantages in early health monitoring by enabling direct, continuous, and highly accurate data monitoring [186]. Halochromic fibers, fabricated via wet spinning and comprising PU and SnO₂, were subjected to hydrophobic treatment and the addition of a pH indicator, enabling their use as a reversible pH smart sensor [4]. CNT@PU nanofibers have been shown to exhibit excellent sensing performance and efficient conductive networks, with applications demonstrated in multimodal sensing, including monitoring human movement, respiration, and pulse [187].

Huang et al. [188] reported that a network of silver nanofibers on wearable fiber textiles coated with conductive PPy cotton knitted fabric has a high sensitivity to different motor activities and can function as a strain sensor. A heterogeneous conductive optical hydrogel fiber sensor device with alternating single and double networks was capable of detecting subtle changes in various body joints and providing feedback through both optical and electrical signals (Fig. 19a) [46]. This approach, which reflects human body movement states via color changes in a heterogeneous structure, is well-suited for health management and related applications.

Thermal sensors can detect local temperature changes in biological tissues accurately and in real time, which is crucial for assessing complex health conditions and offers the possibility for developing smart healthcare systems [189]. As illustrated in Fig. 19b, PU/graphene@PEDOT:PSS fibers integrated with a Bluetooth transmission module can monitor human body temperature [34]. This thermal-responsive composite fiber enables real-time temperature monitoring and relays the data to relevant individuals or caregivers via mobile phones. This system is also applicable for telemedicine, particularly for the prevention and control of outbreaks, such as the COVID-19 pandemic.

As depicted in Fig. 19c, PVA-based hydrogel fibers featuring a nanophase separation network and hierarchical structure were fabricated using conductive tetraphenylamine as a proton trapper [190]. These fibers exhibited a strain monitoring range of up to 660%, which is attributed to the competitive formation of a nanocrystalline domain via a hydrogen-bonding network. The large deformation response renders them suitable for human motion tracking, high-precision pulse-wave detection, and password transmission. As illustrated in Fig. 19d, carbon hybrid fiber sensors demonstrate high sensitivity and durability, enabling their use as sensors on the lumbar and cervical spine to detect real-time

sitting signals to guide healthy lifestyles and facilitate the application of flexible electronic instruments for monitoring human health [47].

On the basis of the practical applications of smart sensors and the development trends of SPFs, it is anticipated that in the near future, smart sensor devices will evolve from “wearing” to “wearing and sensing” and offer a multitude of functions in our daily lives.

5.7 Water Treatment

Many developing countries face a scarcity of clean water, which may stem from inadequate wastewater treatment or the direct discharge of sewage that fails to meet environmental safety standards, thereby contaminating marine environments and posing a threat to the natural conditions upon which human survival depends [191–193]. SPFs can change their wettability in response to external stimuli and are extensively employed in water treatment filters owing to their high specific surface areas, interconnected nanopore structures, tunable pore sizes, and ease of surface texturing and chemical modification [192, 194]. Owing to the hydrophobic and lipophilic properties of a smart composite fabric (DSR-CZPP), when the pH of an aqueous methylene blue (MB) solution was slowly adjusted to 2 and irradiated with UV light for 1 h, the color of the solution faded, and the solution gradually rotated [195]. When oil was added to the solution, UV irradiation resulted in the catalytic degradation of MB by DSR-CZPP, and the interaction between UV irradiation and low pH transformed the interface from hydrophilic to oleophobic.

pH-responsive polymer fibers can switch between hydrophobic and hydrophilic states, enabling the use of a single membrane to control the separation of oil and water, thereby simplifying filtration units and reducing material costs [196]. pH-responsive poly(dimethyl siloxane)-block-poly(4-vinylpyridine) copolymer films exhibit a well-defined porous structure and pH-switchable oil/water wettability, which enables the effective separation of oil or water from lamellar oil/water mixtures under gravity [197]. A dual pH- and moisture-responsive polyimide (PI) nanofibrous membrane with high permeate flux and stability, designed for water treatment [196]. The novel membrane exhibited superhydrophobicity in air and superoleophobicity in neutral aqueous environments (pH 6.5). However, in basic aqueous solutions (pH 12), the membrane exhibits hydrophilic and super-oleophobic properties, enabling water permeation during oil–water separation.

Currently, most oil–water separation membranes are non-biodegradable and rely on toxic solvents [198]. Growing environmental concerns have driven research into biodegradable, eco-friendly alternatives. These materials reduce pollution, support sustainability, and align with green chemistry

principles. Optimizing their design and fabrication is key to addressing water pollution.

5.8 Others

SPFs technology has diverse and extensive applications and has contributed to the development of advanced systems and smart devices. The domains of artificial muscles and soft robots [17] represent highly multidisciplinary areas of research that have undergone swift advancements in recent years [199].

Polydopamine-coated LCE microfibers were developed to mimic biological muscles to achieve rapid contraction under NIR irradiation and were used to drive a 3D-printed arm model to complete a weightlifting action and return to its original state when the NIR source was turned off [200]. These findings demonstrate the potential applications of light-responsive polymer fibers in the field of biomimetic robots that are remotely controlled by a near-infrared laser. The artificial arm simulated the fast contraction of the human triceps muscle through the introduction of LM, which imparted electrothermal responsiveness to LCE fibers [100]. Electrothermal-responsive LM-LCE fibers were prepared and could achieve both an ultrafast contraction rate and a large contraction ratio [100].

Obtaining energy from the widespread water cycle is a promising approach to power generation [201]. Smart textiles can be used as ideal carriers for aqueous voltaic techniques. A plant-inspired [202] asymmetric hygroscopic evaporative recycling fabric generator provides a sustainable and high-performance hydropower solution by efficiently absorbing and expelling water through the micro/nanochannels inside it, enabling a continuous flow of water while driving the redox reaction of the metal electrodes to produce ion-directed motion and enhance the ionic current density [201].

6 Summary and Outlook

SPFs can sensitively perceive and respond to subtle changes in the external environment, a capability derived from their multiscale fine structures, as well as their unique thermal, pH, light, electricity, moisture, magnetic field, and multiple stimuli-responsive properties. This review summarized various stimuli-responsive SPFs and their broad application potential. Meanwhile, artificial intelligence profoundly impacts human life, and interactive SPFs are regarded as the next generation of fiber materials. Along this line, SPFs can potentially impact various interdisciplinary areas, including smart medicine, environmental protection, and robotics. Physical and chemical stimuli-responsive properties have made remarkable progress in

many aspects, but the preparation of multidimensional SPFs by harnessing biologically stimuli-responsive properties and printed organoids represents a promising future trend.

The primary challenge in the development of SPFs lies in optimizing their fabrication processes to ensure that they maintain excellent microstructural integrity and microscopic topography while achieving finer diameters, higher chain orientation, fewer structural defects, and superior stimuli-responsive properties, all with minimal energy consumption for realizing complex functionalities. Portable electronic devices and human–machine interface electrodes based on SPFs can be woven into wearable textiles, which are expected to play a pivotal role in intelligent monitoring, smart healthcare, and smart living in the future.

To summarize, although certain challenges exist in the preparation, microstructural design, and smart and multifunctional applications of SPFs, their enormous application potential and growing industrial demand are driving their rapid development. With progress in scientific research and technology and the steady increase in market demand, the industrialization of SPFs is accelerating, suggesting that these materials will soon play vital roles in our daily lives. However, researchers should consider the potential environmental impact of SPFs and develop more efficient production processes and eco-friendly materials to protect the natural environment.

Acknowledgements This work is funded by the National Natural Science Foundation of China (Grant No. 92271112).

Funding National Natural Science Foundation of China, 92271112, Yanju Liu.

Declarations

Conflicts of interest There are no competing interests to declare.

References

- Chen C, Feng J, Li J, Guo Y, Shi X, Peng H. Functional fiber materials to smart fiber devices. *Chem Rev.* **2023**;123:613.
- Liu X, Yao X, Ou Yang Q, Oliveira AL, Yan L, Zhang Y. Nanofiber scaffold-based tissue engineering for the treatment of acute liver failure. *Adv Fiber Mater.* **2024**;6:686.
- Huang Z, An H, Guo H, Ji S, Gu Q, Gu Z, Wen Y. An asymmetric nanofiber with rapid temperature responsive detachability inspired by andrias davidianus for full-thickness skin wound healing. *Adv Fiber Mater.* **2024**;6:473.
- Hong T, Choi YK, Lim T, Seo K, Jeong S-M, Ju S. Elastic halochromic fiber as a reversible pH sensor. *Adv Mater Technol.* **2021**;6:2001058.
- Yang Y, Zhang X, Valenzuela C, Bi R, Chen Y, Liu Y, Zhang C, Li W, Wang L, Feng W. High-throughput printing of customized structural-color graphics with circularly polarized reflection and mechanochromic response. *Matter.* **2024**;7:2091.
- Luo L, Zhang F, Wang L, Liu Y, Leng J. Recent advances in shape memory polymers: multifunctional materials, multiscale structures, and applications. *Adv Funct Mater.* **2024**;34:2312036.
- He Y, Liu Q, Tian M, Zhang X, Qu L, Fan T, Miao J. Highly conductive and elastic multi-responsive phase change smart fiber and textile. *Compos Commun.* **2023**;44: 101772.
- Li G, Hong G, Dong D, Song W, Zhang X. Multiresponsive graphene-aerogel-directed phase-change smart fibers. *Adv Mater.* **2018**;30:1801754.
- Zheng X, Liu X, Zha L. Fabrication of ultrafast temperature-responsive nanofibrous hydrogel with superelasticity and its ‘on–off’ switchable drug releasing capacity. *J Appl Polym Sci.* **2021**;138:50280.
- Hou Y, Gao L, Feng S, Chen Y, Xue Y, Jiang L, Zheng Y. Temperature-triggered directional motion of tiny water droplets on bioinspired fibers in humidity. *Chem Comm.* **2013**;49:5253–5255.
- Li X, Sun Y, Wang S, Tian G, Yang T, Huang L, Ao Y, Lan B, Zhang J, Xu T, Liu Y, Jin L, Yang W, Deng W. Body temperature-triggered adhesive ionic conductive hydrogels for bioelectrical signal monitoring. *Chem Eng J.* **2024**;498: 155195.
- Chen Y, Valenzuela C, Zhang X, Yang X, Wang L, Feng W. Light-driven dandelion-inspired microfiers. *Nat Commun.* **2023**;14:3036.
- Cheng Q, Lu X, Tai Y, Luo T, Yang R. Light-driven microrobots for targeted drug delivery. *ACS Biomater Sci.* **2024**;10:5562.
- Guo W, Lu CH, Orbach R, Wang F, Qi X-J, Ceconello A, Seliktar D, Willner I. pH-stimulated DNA hydrogels exhibiting shape-memory properties. *Adv Mater.* **2015**;27:73.
- Park J, Yoo JW, Seo HW, Lee Y, Suhr J, Moon H, Koo JC, Choi HR, Hunt R, Kim KJ, Kim SH, Nam JD Electrically controllable twisted-coiled artificial muscle actuators using surface-modified polyester fibers. *Smart Mater Struct.* **2017**;26:035048.
- Wang C, Wang L, Zhang Z, Zhang N, Huang YA. Water-driven shape memory nanocomposite fibers for actuators. *Polym Compos.* **2023**;44:4215.
- Ma S, Xue P, Tang Y, Bi R, Xu X, Wang L, Li Q. Responsive soft actuators with MXene nanomaterials. *Responsive Mater.* **2024**;2: e20230026.
- Huang C, Soenen SJ, Rejman J, Trekker J, Chengxun L, Lagae L, Ceelen W, Wilhelm C, Demeester J, De Smedt SC. Magnetic electrospun fibers for cancer therapy. *Adv Funct Mater.* **2012**;22:2479.
- Gz W, Panahi-Sarmad M, Xi X, Dong K, Mei X, Sm Li, Rq Li, Xi H. Synthesis and properties of multistimuli responsive shape memory polyurethane bioinspired from α -Keratin hair. *Adv Mater Technol.* **2021**;6:2001275.
- Yan S, Zhang F, Luo L, Wang L, Liu Y, Leng J. Shape memory polymer composites: 4D printing, smart structures, and applications. *Research.* **2023**;6:0234.
- Ye G, Yang Y, Yuan W, Gu J, Li S, Li Q, Li Z. Multistimuli-responsive room-temperature phosphorescence: adjustable electrostatic interactions and the corresponding accurate molecular packing. *ACS Mater Lett.* **2024**;6:4639.
- Choi CH, Yi H, Hwang S, Weitz DA, Lee CS. Microfluidic fabrication of complex-shaped microfibers by liquid template-aided multiphase microflow. *Lab Chip.* **2011**;11:1477.
- Wang L, Ma J, Guo T, Zhang F, Dong A, Zhang S, Liu Y, Yuan H, Leng J. Control of surface wrinkles on shape memory PLA/PPDO micro-nanofibers and their applications in drug release and anti-scarring. *Adv Fiber Mater.* **2023**;5:632.
- Nasajpour A, Mostafavi A, Chlanda A, Rinoldi C, Sharifi S, Ji MS, Ye M, Jonas SJ, Swieszkowski W, Weiss PS, Khademhosseini A, Tamayol A. Cholesteryl ester liquid crystal

- nanofibers for tissue engineering applications. *ACS Mater Lett.* **2020**;2:1067.
25. Mao Y, Chen M, Guidoin R, Li Y, Wang F, Brochu G, Zhang Z, Wang L. Potential of a facile sandwiched electrospun scaffold loaded with ibuprofen as an anti-adhesion barrier. *Mater.* **2021**;118: 111451.
 26. Wang J, Xiong H, Zhu T, Liu Y, Pan H, Fan C, Zhao X, Lu WW. Bioinspired multichannel nerve guidance conduit based on shape memory nanofibers for potential application in peripheral nerve repair. *ACS Nano.* **2020**;14:12579.
 27. Liang Q, Zhang D, Wu Y, Chen S, Han Z, Wang B, Wang H. Self-stretchable fiber liquid sensors made with bacterial cellulose/carbon nanotubes for smart diapers. *ACS Appl Mater Interfaces.* **2022**;14:21319.
 28. Duan M, Wang X, Xu W, Ma Y, Yu J. Electro-thermochromic luminescent fibers controlled by self-crystallinity phase change for advanced smart textiles. *ACS Appl Mater.* **2021**;13:57943.
 29. Raza A, Ding B, Zainab G, El-Newehy M, Al-Deyab SS, Yu J. In situ cross-linked superwetting nanofibrous membranes for ultrafast oil–water separation. *J Mater Chem A.* **2014**;2:10137.
 30. Yang H, Guo M. Bioinspired polymeric helical and superhelical microfibers via microfluidic spinning. *Macromol Rapid Commun.* **2019**;40:1900111.
 31. Johnson CDL, Ganguly D, Zuidema JM, Cardinal TJ, Ziembra AM, Kearns KR, McCarthy SM, Thompson DM, Ramanath G, Borca-Tasciuc DA, Dutz S, Gilbert RJ. Injectable, magnetically orienting electrospun fiber conduits for neuron guidance. *ACS Appl Mater.* **2019**;11:356.
 32. Zhang Z, Bolshakov A, Han J, Zhu J, Yang K-L. Electrospun core-sheath fibers with a uniformly aligned polymer network liquid crystal (PNLC). *ACS Appl Mater.* **2023**;15:14800.
 33. Wang L, Zhang F, Liu Y, Leng J. Shape memory polymer fibers: materials, structures, and applications. *Adv Fiber Mater.* **2022**;4:5.
 34. Fan W, Liu T, Wu F, Wang S, Ge S, Li Y, Liu J, Ye H, Lei R, Wang C, Che Q, Li Y. An antisweat interference and highly sensitive temperature sensor based on poly (3,4-ethylenedioxythiophene)-poly (styrenesulfonate) fiber coated with polyurethane/graphene for real-time monitoring of body temperature. *ACS Nano.* **2023**;17:21073.
 35. Liu Y, Wang L, Liu Y, Zhang F, Leng J. Recent progress in shape memory polymer composites: driving modes, forming technologies, and applications. *Compos Commun.* **2024**;51: 102062.
 36. Leng J, Lan X, Liu Y, Du S. Shape-memory polymers and their composites: stimulus methods and applications. *Prog Mater Sci.* **2011**;56:1077.
 37. Xiao X, Kong D, Qiu X, Zhang W, Liu Y, Zhang S, Zhang F, Hu Y, Leng J. Shape memory polymers with high and low temperature resistant properties. *Sci Rep.* **2015**;5:14137.
 38. Xu L, Zhao J, Shi M, Liu J, Wang Z. Thermodynamic properties of TPI shape memory polymer composites reinforced by GO/SiO₂ modified carbon fiber. *Compos Sci Technol.* **2022**;226: 109551.
 39. Sabzi M, Ranjbar-Mohammadi M, Zhang Q, Kargozar S, Leng J, Akhtari T, Abbasi R. Designing triple-shape memory polymers from a miscible polymer pair through dual-electrospinning technique. *J Appl Polym Sci.* **2019**;136:47471.
 40. Wang K, Jia YG, Zhao C, Zhu XX. Multiple and two-way reversible shape memory polymers: design strategies and applications. *Prog Mater Sci.* **2019**;105: 100572.
 41. Xie T. Tunable polymer multi-shape memory effect. *Nature.* **2010**;464:267–70.
 42. Zhao Q, Qi HJ, Xie T. Recent progress in shape memory polymer: new behavior, enabling materials, and mechanistic understanding. *Prog Polym Sci.* **2015**;49–50:79.
 43. Cao H, Duan L, Zhang Y, Cao J, Zhang K. Current hydrogel advances in physicochemical and biological response-driven biomedical application diversity. *Signal Transduct Target Ther.* **2021**;6:426.
 44. Gholamali I. Stimuli-responsive polysaccharide hydrogels for biomedical applications: a review. *Regen Eng Transl Med.* **2021**;7:91.
 45. Khan MUA, Aslam MA, Abdullah MFB, Al-Arjan WS, Stojanovic GM, Hasan A. Hydrogels: classifications, fundamental properties, applications, and scopes in recent advances in tissue engineering and regenerative medicine—a comprehensive review. *Arab J Chem.* **2024**;17: 105968.
 46. Zhang HM, Wang YP, Zhang SF, Niu WB. Heterogeneous structural color conductive photonic organohydrogel fibers with alternating single and dual networks. *ACS Appl Mater Inter.* **2022**;14:54936.
 47. Liu H, Chen Z, Lin X, Zhang X, Cai Y, Zhang Y, Sun B, Mei X, Lyu W, Kaner RB, Zhu M, Liao Y. A nanophase separation strategy toward organohydrogel fibrous sensors with ultralow detection limit and high strain sensitivity. *Chem Mater.* **2024**;36:6100.
 48. Saleh TA, Fadillah G, Ciptawati E. Smart advanced responsive materials, synthesis methods and classifications: from lab to applications. *J Polym Res.* **2021**;28:197.
 49. Qiao S, Wang H. Temperature-responsive polymers: synthesis, properties, and biomedical applications. *Nano Res.* **2018**;11:5400.
 50. Lan R, Shen W, Yao W, Chen J, Chen X, Yang H. Bioinspired humidity-responsive liquid crystalline materials: from adaptive soft actuators to visualized sensors and detectors. *Mater Horiz.* **2023**;10:2824.
 51. Zhang Z, Wang Q, Li Y, Wang C, Yang X, Shang L. Cholesteric cellulose liquid crystal fibers by direct drawing. *Research.* **2024**;7:0527.
 52. Wang Y, Liu J, Yang SJAPR. Multi-functional liquid crystal elastomer composites. *Appl Phys Rev.* **2022**;9:011301.
 53. Wolinski TR, Czaplak A, Ertman S, Tefelska M, Domanski AW, Wojcik J, Nowinowski-Kruszelnicki E, Dabrowski R. Photonic liquid crystal fibers for sensing applications. *IEEE Trans Instrum Meas.* **2008**;57:1796.
 54. Sun J, Wang C, Liu Y, Liang X, Wang Z. Liquid crystal elastomer composites for soft actuators. *Int J Smart Nano Mater.* **2023**;14:440.
 55. Shi S, Si Y, Han Y, Wu T, Iqbal MI, Fei B, Li RKY, Hu J, Qu J. Recent progress in protective membranes fabricated via electrospinning: advanced materials, biomimetic structures, and functional applications. *Adv Mater.* **2022**;34:2107938.
 56. Xu H, Yagi S, Ashour S, Du L, Hoque ME, Tan L. A review on current nanofiber technologies: electrospinning, centrifugal spinning, and electro-centrifugal spinning. *Macromol Mater.* **2023**;308:2200502.
 57. Lee KY, Jeong L, Kang YO, Lee SJ, Park WH. Electrospinning of polysaccharides for regenerative medicine. *Adv Drug Del Rev.* **2009**;61:1020.
 58. Jin B, Yu Y, Lou C, Zhang X, Gong B, Chen J, Chen X, Zhou Z, Zhang L, Xiao J, Xue J. Combining a density gradient of biomacromolecular nanoparticles with biological effectors in an electrospun fiber-based nerve guidance conduit to promote peripheral nerve repair. *Adv Sci.* **2023**;10:2203296.
 59. Wang B, Li B, Xiong J, Li CY. Hierarchically ordered polymer nanofibers via electrospinning and controlled polymer crystallization. *Macromolecules.* **2008**;41:9516.
 60. Zhuo H. Coaxial electrospun polyurethane core-shell nanofibers for shape memory and antibacterial nanomaterials. *Express Polym Lett.* **2011**;5:182.
 61. Jin Y, Yang D, Kang D, Jiang X. Fabrication of necklace-like structures via electrospinning. *Langmuir.* **2010**;26:1186.

62. Chen H, Wang N, Di J, Zhao Y, Song Y, Jiang L. Nanowire-in-microtube structured core/shell fibers via multifluidic coaxial electrospinning. *Langmuir*. **2010**;26:11291.
63. Holzmeister A, Greiner A, Wendorff JH. "Barbed nanowires" from polymers via electrospinning. *Polym Eng Sci*. **2008**;49:148.
64. Zhao Y, Cao X, Jiang L. Bio-mimic multichannel microtubes by a facile method. *J Am Chem Soc*. **2007**;129:764.
65. Guan Y, Agra-Kooijman DM, Fu S, Jákli A, West JL. Responsive liquid-crystal-clad fibers for advanced textiles and wearable sensors. *Adv Mater*. **2019**;31:1902168.
66. Wu Y, An Q, Yin J, Hua T, Xie H, Li G, Tang H. Liquid crystal fibers produced by using electrospinning technique. *Colloid Polym Sci*. **2008**;286:897.
67. Yan G, Yu J, Qiu Y, Yi X, Lu J, Zhou X, Bai X. Self-assembly of electrospun polymer nanofibers: a general phenomenon generating honeycomb-patterned nanofibrous structures. *Langmuir*. **2011**;27:4285.
68. Wang R, Xie L, Zhang Z, Sun H, Xiao Y. Mussel-inspired wet-spun conductive fibers for stretchable electronics. *Compos Commun*. **2025**;53: 102171.
69. Rohani Shirvan A, Nouri A, Sutti A. A perspective on the wet spinning process and its advancements in biomedical sciences. *Eur Polym J*. **2022**;181: 111681.
70. Yang Y, Sun J, Liu X, Guo Z, He Y, Wei D, Zhong M, Guo L, Fan H, Zhang X. Wet-spinning fabrication of shear-patterned alginate hydrogel microfibers and the guidance of cell alignment. *Regen Biomater*. **2017**;4:299.
71. Klar V, Orelma H, Rautkoski H, Kuosmanen P, Harlin A. Spinning approach for cellulose fiber yarn using a deep eutectic solvent and an Inclined channel. *ACS Omega*. **2018**;3:10918.
72. Mollahosseini H, Fashandi H, Khoddami A, Zarrebini M, Nikukar H. Recycling of waste silk fibers towards silk fibroin fibers with different structures through wet spinning technique. *J Cleaner Prod*. **2019**;236: 117653.
73. Noor N, Koll J, Scharnagl N, Abetz C, Abetz V. Hollow fiber membranes of blends of polyethersulfone and sulfonated polymers. *Membranes*. **2018**;8:54.
74. Qi X, Liu Y, Yu L, Yu Z, Chen L, Li X, Xia Y. Versatile liquid metal/alginate composite fibers with enhanced flame retardancy and triboelectric performance for smart wearable textiles. *Adv Sci*. **2023**;10:2303406.
75. Song Y, Yu XQ, Chen S. Recent advances in microfluidic fiber-spinning chemistry. *J Polym Sci*. **2023**;62:447.
76. Zhou M, Gong J, Ma J. Continuous fabrication of near-infrared light responsive bilayer hydrogel fibers based on microfluidic spinning. *E-Polymers*. **2019**;19:215.
77. Liu JD, Du XY, Chen S. A phase inversion-based microfluidic fabrication of helical microfibers towards versatile artificial abdominal skin. *Angew Chem Int Ed*. **2021**;60:25089.
78. Guo JH, Yu YR, Wang H, Zhang H, Zhang XX, Zhao YJ. Conductive polymer hydrogel microfibers from multifold microfluidics. *Small*. **2019**;15:1805162.
79. Peng R, Ba F, Li J, Cao J, Zhang R, Liu W-Q, Ren J, Liu Y, Li J, Ling S. Embedding living cells with a mechanically reinforced and functionally programmable hydrogel fiber platform. *Adv Mater*. **2023**;35:2305583.
80. Yu Y, Fu F, Shang L, Cheng Y, Gu Z, Zhao Y. Bioinspired helical microfibers from microfluidics. *Adv Mater*. **2017**;29:1605765.
81. Liu Y, Wu P. Bioinspired hierarchical liquid-metacrylate fibers for chiral optics and advanced textiles. *Adv Funct Mater*. **2020**;30:2002193.
82. Yang CY, Yu YR, Wang XC, Shang LR, Zhao YJ. Programmable knot microfibers from piezoelectric microfluidics. *Small*. **2022**;18:2104309.
83. Liu H, Wang Y, Yin W, Yuan H, Guo T, Meng T. Highly efficient water harvesting of bioinspired spindle-knotted microfibers with continuous hollow channels. *J Mater Chem A*. **2022**;10:7130.
84. Huang C, Soenen SJ, Rejman J, Lucas B, Braeckmans K, Demeester J, De Smedt SC. Stimuli-responsive electrospun fibers and their applications. *Chem Soc Rev*. **2011**;40:2417–34.
85. Liu L, Xu W, Ding Y, Agarwal S, Greiner A, Duan G. A review of smart electrospun fibers toward textiles. *Compos Commun*. **2020**;22: 100506.
86. Zhang F, Zhang Z, Liu Y, Cheng W, Huang Y, Leng J. Thermo-setting epoxy reinforced shape memory composite microfiber membranes: fabrication, structure and properties. *Compos Part A Appl Sci Manuf*. **2015**;76:54.
87. Leones A, Sonseca A, López D, Fiori S, Peponi L. Shape memory effect on electrospun PLA-based fibers tailoring their thermal response. *Eur Polym J*. **2019**;117:217.
88. Tseng LF, Mather PT, Henderson JH. Shape-memory-actuated change in scaffold fiber alignment directs stem cell morphology. *Acta Biomater*. **2013**;9:8790.
89. Bao M, Lou X, Zhou Q, Dong W, Yuan H, Zhang Y. Electrospun biomimetic fibrous scaffold from shape memory polymer of PDLA-co-TMC for bone tissue engineering. *ACS Appl Mater*. **2014**;6:2611.
90. Schoeller J, Itef F, Wuertz-Kozak K, Fortunato G, Rossi RM. pH-responsive electrospun nanofibers and their applications. *Polym Rev*. **2022**;62:351.
91. Tamayol A, Akbari M, Zilberman Y, Comotto M, Lesha E, Serex L, Bagherifard S, Chen Y, Fu G, Ameri SK, Ruan W, Miller EL, Dokmeci MR, Sonkusale S, Khademhosseini A. Flexible pH-sensing hydrogel fibers for epidermal applications. *Adv Health Mater*. **2016**;5:711.
92. Yuan Z, Zhao J, Zhu W, Yang Z, Li B, Yang H, Zheng Q, Cui W. Ibuprofen-loaded electrospun fibrous scaffold doped with sodium bicarbonate for responsively inhibiting inflammation and promoting muscle wound healing in vivo. *Biomater Sci*. **2014**;2:502.
93. Tan S, Han J, Yuan X, Song Z, Gao L, Gao J, Wang L. Epigallocatechin gallate-loaded pH-responsive dressing with effective antioxidant, antibacterial and anti-biofilm properties for wound healing. *Mater Des*. **2023**;227: 111701.
94. He CW, Parowatkin M, Mailänder V, Flechtner-Mors M, Ziener U, Landfester K, Crespy D. Sequence-controlled delivery of peptides from hierarchically structured nanomaterials. *ACS Appl Mater*. **2017**;9:3885.
95. Zhao S, Mehta AS, Zhao M. Biomedical applications of electrical stimulation. *Cell Mol Life Sci*. **2020**;77:2681.
96. Xiang XW, Liu HT, Liu W, Yan ZY, Zeng YL, Wang YJ, Liu J, Chen YC, Yu SX, Zhu CH, Tao XN, Wang C, Wu JT, Du Y, Xu XX, Gao H, Jiu Y, Ma J, Qiu J, Chang L, Jing G, Liu KF, Liu YJ. Revolutionizing wound healing: ultrashort pulse electric fields in seconds for highly aligned extracellular matrix and efficient cell migration. *Chem Eng J*. **2023**;471: 144267.
97. Borges MHR, Nagay BE, Costa RC, Souza JGS, Mathew MT, Barão VAR. Recent advances of polypyrrole conducting polymer film for biomedical application: toward a viable platform for cell-microbial interactions. *Adv Colloid Interface Sci*. **2023**;314: 102860.
98. Lu H, Yao Y, Yin J, Lin L. Functionally graded carbon nanotube and nafion/silica nanofiber for electrical actuation of carbon fiber reinforced shape memory polymer. *Pigment Resin Technol*. **2016**;45:93.
99. Zhang F, Xia Y, Wang L, Liu L, Liu Y, Leng J. Conductive shape memory microfiber membranes with core-shell structures and electroactive performance. *ACS Appl Mater*. **2018**;10:35526.
100. Sun J, Wang Y, Liao W, Yang Z. Ultrafast, high-contractile electrothermal-driven liquid crystal elastomer fibers towards artificial muscles. *Small*. **2021**;17:2103700.

101. Peng L, Liu Y, Gong J, Zhang K, Ma J. Continuous fabrication of multi-stimuli responsive graphene oxide composite hydrogel fibres by microfluidics. *RSC Adv.* **2017**;7:19243.
102. Liu C, Wang Z, Wei X, Chen B, Luo Y. 3D printed hydrogel/PCL core/shell fiber scaffolds with NIR-triggered drug release for cancer therapy and wound healing. *Acta Biomater.* **2021**;131:314.
103. Reinhart MB, Huntington CR, Blair LJ, Heniford BT, Augenstein VA. Indocyanine green: historical context, current applications, and future considerations. *Surg Innov.* **2016**;23:166.
104. Dong Y, Fu S, Yu J, Li X, Ding B. Emerging smart micro/nanofiber-based materials for next-generation wound dressings. *Adv Funct Mater.* **2024**;34:2311199.
105. Bai Y, Zhou Z, Zhu Q, Lu S, Li Y, Ionov L. Electrospun cellulose acetate nanofibrous composites for multi-responsive shape memory actuators and self-powered pressure sensors. *Carbohydr Polym.* **2023**;313: 120868.
106. Wei X, Chen L, Wang Y, Sun Y, Ma C, Yang X, Jiang S, Duan G. An electrospinning anisotropic hydrogel with remotely-controlled photo-responsive deformation and long-range navigation for synergist actuation. *Chem Eng J.* **2022**;433: 134258.
107. Yang H, Wu D, Zheng S, Yu Y, Ren L, Li J, Ke H, Lv P, Wei Q. Fabrication and photothermal actuation performances of electrospun carbon nanotube/liquid crystal elastomer blend yarn actuators. *ACS Appl Mater Inter.* **2024**;16:9313.
108. Zou H, Weder C, Simon YC. Shape-memory polyurethane nanocomposites with single layer or bilayer oleic acid-coated Fe₃O₄ nanoparticles. *Macromol Mater Eng.* **2015**;300:885.
109. Chen Z, Feng T, Cheng X. Magnetic nanoparticles coated with a molecularly imprinted polymer via manganese-doped ZnS: Mn quantum dots for the determination of triflumuron. *Polym-Plast Tech Mat.* **2024**;63:1096.
110. Battesti R, Beard J, Böser S, Bruyant N, Budker D, Crooker SA, Daw EJ, Flambaum VV, Inada T, Irastorza IG, Karbstein F, Kim DL, Kozlov MG, Melhem Z, Phipps A, Pugnati P, Rikken G, Rizzo C, Schott M, Semertzidis YK, ten Kate HHJ, Zavattini G. High magnetic fields for fundamental physics. *Phys Rep.* **2018**;765–766:1.
111. Gong T, Li W, Chen H, Wang L, Shao S, Zhou S. Remotely actuated shape memory effect of electrospun composite nanofibers. *Acta Biomater.* **2012**;8:1248.
112. Islam MS, Molley TG, Hung TT, Sathish CI, Putra VDL, Jalandhra GK, Ireland J, Li Y, Yi J, Krusic JJ, Kilian KA. Magnetic nanofibrous hydrogels for dynamic control of stem cell differentiation. *ACS Appl Mater.* **2023**;15:50663.
113. Wang L, Li T, Wang Z, Hou J, Liu S, Yang Q, Yu L, Guo W, Wang Y, Guo B, Huang W, Wu Y. Injectable remote magnetic nanofiber/hydrogel multiscale scaffold for functional anisotropic skeletal muscle regeneration. *Biomaterials.* **2022**;285: 121537.
114. Zhang B, Yu Q, Liu Y. Polarization of stem cells directed by magnetic field-manipulated supramolecular polymeric nanofibers. *ACS Appl Mater Interfaces.* **2021**;13:9580.
115. Wang Y, Wang Z, Lu Z, Jung de Andrade M, Fang S, Zhang Z, Wu J, Baughman RH. Humidity- and water-responsive torsional and contractile lotus fiber yarn artificial muscles. *ACS Appl Mater Inter.* **2021**;13:6642.
116. Du B, Wang X, Xia Y, Wu Y, Wu B, Huang S. Hygroscopic tunable multishape memory effect in cellulosic macromolecular networks with a supramolecular mesophase. *ACS Macro Lett.* **2023**;12:835.
117. Liu W, Zhao W, Xie K, Li XF, Wang Y, Kong D, Liu Y, Leng J. Toughening and responsive contractile shape memory fibrous membrane via water for mechanically active wound dressing. *Adv Fiber Mater.* **2024**;6:1942.
118. Venkatesan H, Chen J, Liu H, Kim Y, Na S, Liu W, Hu J. Artificial spider silk is smart like natural one: having humidity-sensitive shape memory with superior recovery stress. *Mater Chem Front.* **2019**;3:2472.
119. Xu X, Wang Z, Su Y, Zhang K, Li M, Zhang Q, Zhang S, Zhao Y, Ke Q, Hu H, Young RJ, Zhu S, Hu J. Biomimetic design of hydration-responsive silk fibers and their role in actuators and self-modulated textiles. *Adv Funct Mater.* **2024**;34:2401732.
120. Xu C, Jiang Z, Zhong T, Chen C, Ren W, Sun T, Fu F. Multi-strand fibers with hierarchical helical structures driven by water or moisture for soft actuators. *ACS Omega.* **2023**;8:2243.
121. Shen X, Hu Q, Akbarzadeh A, Shi C, Pang Z, Ge M. Multi-stimuli-responsive composite fibers based on luminescent ceramics for UV/heat detection and anti-counterfeiting. *J Mater Chem C.* **2021**;9:15175.
122. Wang Q, Zhang L, Zhong Y, Xu H, Mao Z. Hydrogel fiber actuators prepared by shell-core structure for high-performance water/light dual response. *Adv Fiber Mater.* **2024**;6:1887.
123. Liu L, Yang T, Wang S, Jia W, Liu Y, Jiao K, Yan Y, Yang Y, Jiang X, Li C, Cheng Z, Liu G, Luo Y. Preparation and design of intelligent multi-response PTMC/PVP composite nanofibrous dressing to promote wound closure and its applications in diabetic wounds. *Chem Eng J.* **2024**;495: 153872.
124. Wei Z, Yang J, Long S, Zhang G, Wang X. Smart and in-situ formation electrospun fibrous membrane for the control of antimicrobial efficacy. *Smart Mater Med.* **2021**;2:87–95.
125. Wei H, Zhang F, Zhang D, Liu Y, Leng J. Shape-memory behaviors of electrospun chitosan/poly(ethylene oxide) composite nanofibrous membranes. *J Appl Polym Sci.* **2015**;132:42532.
126. Yao Y, Wang J, Lu H, Xu B, Fu Y, Liu Y, Leng J. Thermosetting epoxy resin/thermoplastic system with combined shape memory and self-healing properties. *Smart Mater Struct.* **2016**;25: 015021.
127. Cheng F, Gao J, Wang L, Hu X. Composite chitosan/poly(ethylene oxide) electrospun nanofibrous mats as novel wound dressing matrixes for the controlled release of drugs. *J Appl Polym Sci.* **2015**;132:42060.
128. Aguilar LE, Unnithan AR, Amarjargal A, Tiwari AP, Hong ST, Park CH, Kim CS. Electrospun polyurethane/Eudragit® L100–55 composite mats for the pH dependent release of paclitaxel on duodenal stent cover application. *Int J Pharm.* **2015**;478:1.
129. Nakielski P, Pawlowska S, Rinoldi C, Ziai Y, De Sio L, Urbanek O, Zembrzycki K, Pruchniewski M, Lanzi M, Salatelli E, Calogero A, Kowalewski TA, Yarin AL, Pierini F. Multifunctional platform based on electrospun nanofibers and plasmonic hydrogel: a smart nanostructured pillow for near-infrared light-driven biomedical applications. *ACS Appl Mater Inter.* **2020**;12:54328.
130. Chen M, Besenbacher F. Light-driven wettability changes on a photoresponsive electrospun mat. *ACS Nano.* **2011**;5:1549.
131. Wang B, Zheng H, Chang M-W, Ahmad Z, Li JS. Hollow polycaprolactone composite fibers for controlled magnetic responsive antifungal drug release. *Colloids Surf B.* **2016**;145:757.
132. Jedlovszky-Hajdu A, Molnar K, Nagy PM, Sinko K, Zrinyi M. Preparation and properties of a magnetic field responsive three-dimensional electrospun polymer scaffold. *Colloids Surf.* **2016**;503:79.
133. Gu X, Mather PT. Water-triggered shape memory of multiblock thermoplastic polyurethanes (TPUs). *RSC Adv.* **2013**;3:15783.
134. Croitoru AM, Karaçelebi Y, Saatcioglu E, Altan E, Ulag S, Aydoğan HK, Sahin A, Motelica L, Oprea O, Tihauan BM, Popescu RC, Savu D, Trusca R, Ficai D, Gunduz O, Ficai A. Electrically triggered drug delivery from novel electrospun poly(lactic acid)/graphene oxide/quercetin fibrous scaffolds for wound dressing applications. *Pharmaceutics.* **2021**;13:957.
135. Zhang N, Cheng H, Han W, Ge F, Yin Y, Wang C. Electrical-triggered multicolor reversible color-changing Ag nanoparticles/reduced graphene oxide/polyurethane conductive fibers. *Macromol Mater.* **2022**;308:2200438.

136. Dallmeyer I, Chowdhury S, Kadla JF. Preparation and characterization of kraft lignin-based moisture-responsive films with reversible shape-change capability. *Biomacromol.* **2013**;14:2354.
137. Alam AKMM, Yapor J, Reynolds M, Li Y. Study of polydiacetylene-poly(ethylene oxide) electrospun fibers used as biosensors. *Materials.* **2016**;9:202.
138. Wang H, Shi C, Yue X, Zhang Z, Zhang Z, Li X, Jin Y. Electricity trigger chameleon core-shell fiber via liquid metal drive thermochromic polyacrylonitrile. *J Alloys Compd.* **2023**;968:172013.
139. Lee GS, Kim JG, Kim JT, Lee CW, Cha S, Choi GB, Lim J, Padmajan Sasikala S, Kim SO. 2D materials beyond post-AI era: smart fibers, soft robotics, and single atom catalysts. *Adv Mater.* **2023**;36:2307689.
140. Kim YJ, Ebara M, Aoyagi T. A smart hyperthermia nanofiber with switchable drug release for inducing cancer apoptosis. *Adv Funct Mater.* **2013**;23:5753.
141. Li S, Wu J, Peng X, Feng XQ. Unlocking the potential of transdermal drug delivery. *Int J Smart Nano Mater.* **2024**;15:432.
142. Wang L, Yang Q, Yang Y, Luo K, Bai R. Porous polyurethane hydrogels incorporated with CMC for eliminating methylene blue from water. *Int J Smart Nano Mater.* **2023**;14:57.
143. Phan PT, Thai MT, Hoang TT, Davies J, Nguyen CC, Phan H-P, Lovell NH, Do TN. Smart textiles using fluid-driven artificial muscle fibers. *Sci Rep.* **2022**;12:11067.
144. Sun C, Luo J, Yan S, Li K, Li Y, Wang H, Hou C, Zhang Q. Thermally responsive fibers for versatile thermoactivated protective fabrics. *Adv Funct Mater.* **2022**;33:2211035.
145. Li JJ, Zhou YN, Luo ZH. Smart fiber membrane for pH-induced oil/water separation. *ACS Appl Mater Interfaces.* **2015**;7:19643.
146. Shang S, Zhang Q, Wang H, Li Y. Facile fabrication of magnetically responsive PDMS fiber for camouflage. *J Colloid Interface Sci.* **2016**;483:11–16.
147. Yin Z, Jian M, Wang C, Xia K, Liu Z, Wang Q, Zhang M, Wang H, Liang X, Liang X, Long Y, Yu X, Zhang Y. Splash-resistant and light-weight silk-sheathed wires for textile electronics. *Nano Lett.* **2018**;18:7085.
148. Zhang XA, Yu S, Xu B, Li M, Peng Z, Wang Y, Deng S, Wu X, Wu Z, Ouyang M, Wang Y. Dynamic gating of infrared radiation in a textile. *Science.* **2019**;363:619.
149. Lu H, Zhang Y, Zhu M, Li S, Liang H, Bi P, Wang S, Wang H, Gan L, Wu XE, Zhang Y. Intelligent perceptual textiles based on ionic-conductive and strong silk fibers. *Nat Commun.* **2024**;15:3289.
150. Liu GY, Agarwal R, Ko KR, Ruthven M, Sarhan HT, Frampton JP. Templated assembly of collagen fibers directs cell growth in 2D and 3D. *Sci Rep.* **2017**;7:9628.
151. Zheng W, Wang Y, Zhang F, Li C, Liu Y, Leng J. Development of shape memory polymers micro/nanofiber membranes in biomedical applications. *Sci Sin Technol.* **2018**;48:811.
152. Ruiter FAA, Sidney LE, Kiick KL, Segal JJ, Alexander C, Rose FRAJ. The electrospinning of a thermo-responsive polymer with peptide conjugates for phenotype support and extracellular matrix production of therapeutically relevant mammalian cells. *Biomater Sci.* **2020**;8:2611.
153. Xiong R, Hua D, Van Hock J, Berdecka D, Léger L, De Munter S, Fraire JC, Raes L, Harizaj A, Sauvage F, Goetgeluk G, Pille M, Aalders J, Belza J, Van Acker T, Bolea-Fernandez E, Si T, Vanhaecke F, De Vos WH, Vandekerckhove B, van Hengel J, Raemdonck K, Huang C, De Smedt SC, Braeckmans K. Photothermal nanofibres enable safe engineering of therapeutic cells. *Nat Nanotechnol.* **2021**;16:1281.
154. Yao S, Yang Y, Li C, Yang K, Song X, Li C, Cao Z, Zhao H, Yu X, Wang X, Wang L-N. Axon-like aligned conductive CNT/GelMA hydrogel fibers combined with electrical stimulation for spinal cord injury recovery. *Bioact.* **2024**;35:534.
155. Niiyama E, Tanabe K, Uto K, Kikuchi A, Ebara M. Shape-memory nanofiber meshes with programmable cell orientation. *Fibers.* **2019**;7:20.
156. Kalayil N, Budar AA, Dave RK. Nanofibers for drug delivery: design and fabrication strategies. *BIO Integr.* **2024**;5:978.
157. Kim YJ, Matsunaga YT. Thermo-responsive polymers and their application as smart biomaterials. *J Mater Chem B.* **2017**;5:4307.
158. He W, Ma Y, Gao X, Wang X, Dai X, Song J. Application of poly(N-isopropylacrylamide) as thermosensitive smart materials. *J Phys Conf Ser.* **2020**;1676:012063.
159. Alavijeh RZ, Shokrollahi P, Barzin J. A thermally and water activated shape memory gelatin physical hydrogel, with a gel point above the physiological temperature, for biomedical applications. *J Mater Chem B.* **2017**;5:2302.
160. Chen X, Li H, Lu W, Guo Y. Antibacterial porous coaxial drug-carrying nanofibers for sustained drug-releasing applications. *Nanomaterials.* **2021**;11:1316.
161. Zhang H, Niu Q, Wang N, Nie J, Ma G. Thermo-sensitive drug controlled release PLA core/PNIPAM shell fibers fabricated using a combination of electrospinning and UV photo-polymerization. *Eur Polym J.* **2015**;71:440.
162. Singh B, Kim J, Shukla N, Lee J, Kim K, Park M-H. Smart delivery platform using core-shell nanofibers for sequential drug release in wound healing. *ACS Appl Bio Mater.* **2023**;6:2314.
163. Slemming-Adamsen P, Song J, Dong M, Besenbacher F, Chen M. In situ cross-linked PNIPAM/gelatin nanofibers for thermo-responsive drug release. *Macromol Mater.* **2015**;300:1226.
164. Tang J, Zhao R, Yin X, Wen Y, Shi Y, Zhu P, Chen Z, Zeng R, Tan L. Programmable release of berberine chloride hydrate from shape memory fibers prepared from core-sheath wet-spinning technology. *J Biomed Nanotechnol.* **2019**;15:1432.
165. Li W, Jiang L, Wu S, Yang S, Ren L, Cheng B, Xia J. A shape-programmable hierarchical fibrous membrane composite system to promote wound healing in diabetic patients. *Small.* **2022**;18:2107544.
166. Singh B, Shukla N, Kim J, Kim K, Park M-H. Stimuli-responsive nanofibers containing gold nanorods for on-demand drug delivery platforms. *Pharmaceutics.* **2021**;13:1319.
167. Wei Z, Lin Q, Yang J, Long S, Zhang G, Wang X. Fabrication of novel dual thermo- and pH-sensitive poly(N-isopropylacrylamide-N-methylolacrylamide-acrylic acid) electrospun ultrafine fibres for controlled drug release. *Mater.* **2020**;115:111050.
168. Lv H, Tang D, Sun Z, Gao J, Yang X, Jia S, Peng J. Electrospun PCL-based polyurethane/HA microfibers as drug carrier of dexamethasone with enhanced biodegradability and shape memory performances. *Colloid Polym Sci.* **2020**;298:103.
169. Zheng M, Yao S, Zhao Y, Wan X, Hu Q, Tang C, Jiang Z, Wang S, Liu Z, Li L. Self-driven electrical stimulation-promoted cancer catalytic therapy and chemotherapy based on an implantable nanofibrous patch. *ACS Appl Mater Inter.* **2023**;15:7855.
170. Sun D, Zhang Z, Chen M, Zhang Y, Amagat J, Kang S, Zheng Y, Hu B, Chen M. Co-immobilization of Ce6 sono/photosensitizer and protonated graphitic carbon nitride on PCL/gelatin fibrous scaffolds for combined sono-photodynamic cancer therapy. *ACS Appl Mater Inter.* **2020**;12:40728.
171. O'Brien FJ. Biomaterials & scaffolds for tissue engineering. *Mater Today.* **2011**;14:88.
172. Xie X, Chen Y, Wang X, Xu X, Shen Y, Khan AR, Aldalbah A, Fetz AE, Bowlin GL, El-Newehy M, Mo X. Electrospinning nanofiber scaffolds for soft and hard tissue regeneration. *J Mater Sci Technol.* **2020**;59:243.
173. Yadav P, Beniwal G, Saxena KK. A review on pore and porosity in tissue engineering. *Mater Today.* **2021**;44:2623.
174. Zhao C, Chen R, Chen Z, Lu Q, Zhu H, Bu Q, Yin J, He H. Bioinspired multifunctional cellulose nanofibril-based in situ liquid wound dressing for multiple synergistic therapy of

- the postoperative infected wound. *ACS Appl Mater Inter.* **2021**;13:51578.
175. Yang CY, Meng Z, He Z, Ma P, Hou Z, Kim K, Lu J, Yang K, Wang G, Wang X. Engineering neuroregenerative microenvironment via aligned hydrogel-assisted magnetic stimulation for complete spinal cord injury repair. *Eng Regen.* **2024**;5:139.
 176. Li P, Sun Z, Wang R, Gong Y, Zhou Y, Wang Y, Liu X, Zhou X, Ouyang J, Chen M, Hou C, Chen M, Tao G. Flexible thermochromic fabrics enabling dynamic colored display. *Front.* **2022**;15:40.
 177. Yang J, Zhang X, Zhang X, Wang L, Feng W, Li Q. Beyond the visible: bioinspired infrared adaptive materials. *Adv Mater.* **2021**;33:2004754.
 178. Wang C, Shi J, Zhang L, Fu S. Asymmetric janus fibers with bistable thermochromic and efficient solar–thermal properties for personal thermal management. *Adv Fiber Mater.* **2024**;6:264.
 179. Li B, Valenzuela C, Liu Y, Zhang X, Yang Y, Chen Y, Wang L, Feng W. Free-standing bacterial cellulose-templated radiative cooling liquid crystal films with self-adaptive solar transmittance modulation. *Adv Funct Mater.* **2024**;34:2402124.
 180. Shen X, Hu Q, Ge M. Fabrication and characterization of multi stimuli-responsive fibers via wet-spinning process. *Spectrochim Acta A.* **2021**;250: 119245.
 181. Xue T, Zhu C, Yu D, Zhang X, Lai F, Zhang L, Zhang C, Fan W, Liu T. Fast and scalable production of crosslinked polyimide aerogel fibers for ultrathin thermoregulating clothes. *Nat Commun.* **2023**;14:8378.
 182. Xue T, Zhu C, Feng X, Wali Q, Fan W, Liu T. Polyimide aerogel fibers with controllable porous microstructure for super-thermal insulation under extreme environments. *Adv Fiber Mater.* **2022**;4:1118.
 183. Shuai L, Guo ZH, Zhang P, Wan J, Pu X, Wang ZL. Stretchable, self-healing, conductive hydrogel fibers for strain sensing and triboelectric energy-harvesting smart textiles. *Nano Energy.* **2020**;78: 105389.
 184. Wu D, Li X, Zhang Y, Cheng X, Long Z, Ren L, Xia X, Wang Q, Li J, Lv P, Feng Q, Wei Q. Novel biomimetic “spider web” robust, super-contractile liquid crystal elastomer active yarn soft actuator. *Adv Sci.* **2024**;11:2400557.
 185. Leal-Junior A, Avellar L, Frizzera A, Marques C. Smart textiles for multimodal wearable sensing using highly stretchable multiplexed optical fiber system. *Sci Rep.* **2020**;10:13867.
 186. Smith AA, Li R, Tse ZTH. Reshaping healthcare with wearable biosensors. *Sci Rep.* **2023**;13:4998.
 187. Qi K, Zhou Y, Ou K, Dai Y, You X, Wang H, He J, Qin X, Wang R. Weavable and stretchable piezoresistive carbon nanotubes-embedded nanofiber sensing yarns for highly sensitive and multimodal wearable textile sensor. *Carbon.* **2020**;170:464.
 188. Hao D, Xu B, Cai Z. Polypyrrole coated knitted fabric for robust wearable sensor and heater. *J Mater Sci Mater Electron.* **2018**;29:9218.
 189. Li Q, Zhang LN, Tao XM, Ding X. Review of flexible temperature sensing networks for wearable physiological monitoring. *Adv Healthc Mater.* **2017**;6:1601371.
 190. Hu Y, Huang T, Zhang H, Lin H, Zhang Y, Ke L, Cao W, Hu K, Ding Y, Wang X, Rui K, Zhu J, Huang W. Ultrasensitive and wearable carbon hybrid fiber devices as robust intelligent sensors. *ACS Appl Mater Inter.* **2021**;13:23905.
 191. Thakur S, Verma A, Kumar V, Jin Yang X, Krishnamurthy S, Coulon F, Thakur VK. Cellulosic biomass-based sustainable hydrogels for wastewater remediation: chemistry and prospective. *Fuel.* **2022**;309: 122114.
 192. Su H, Hu H, Li Z, Yan G, Wang L, Xiang D, Zhao C, Wu Y, Chen J, Wang C. Pre-oxidized PAN nanofibrous membrane to efficiently and continuously separate large-scale viscous oil-in-water emulsions under harsh conditions with ultra-long-term oil-fouling recovery. *Adv Fiber Mater.* **2024**;6:852.
 193. Yang X, Tian Y, Zhou R, Xia F, Gong Y, Zhang C, Ji F, Liu L, Li F, Zhang R, Yu J, Gao T. Bioinspired design of textile-based absorbers: photothermal and electrothermal synergistic conversion for efficient clean-up of heavy oil. *Adv Fiber Mater.* **2024**;6:1446.
 194. Liu H, Zhang L, Huang J, Mao J, Chen Z, Mao Q, Ge M, Lai Y. Smart surfaces with reversibly switchable wettability: concepts, synthesis and applications. *Adv Colloid Interface Sci.* **2022**;300: 102584.
 195. Wang DC, Yang X, Yu HY, Gu J, Qi D, Yao J, Ni Q. Smart nonwoven fabric with reversibly dual-stimuli responsive wettability for intelligent oil-water separation and pollutants removal. *J Hazard Mater.* **2020**;383: 121123.
 196. Ma W, Samal SK, Liu Z, Xiong R, De Smedt SC, Bhushan B, Zhang Q, Huang C. Dual pH- and ammonia-vapor-responsive electrospun nanofibrous membranes for oil-water separations. *J Membr Sci.* **2017**;537:128.
 197. Li JJ, Zhou YN, Jiang ZD, Luo ZH. Electrospun fibrous mat with pH-switchable superwettability that can separate layered oil/water mixtures. *Langmuir.* **2016**;32:13358.
 198. Oh S, Bang J, Jin HJ, Kwak HW. Green fabrication of underwater superoleophobic biopolymeric nanofibrous membranes for effective oil–water separation. *Adv Fiber Mater.* **2023**;5:603.
 199. Chen Y, Valenzuela C, Liu Y, Yang X, Yang Y, Zhang X, Ma S, Bi R, Wang L, Feng W. Biomimetic artificial neuromuscular fiber bundles with built-in adaptive feedback. *Matter.* **2024**;8:101904.
 200. He Q, Wang Z, Wang Y, Wang Z, Li C, Annappooranan R, Zeng J, Chen R, Cai S. Electrospun liquid crystal elastomer microfiber actuator. *Sci Robot.* **2021**;6:eabi9704.
 201. Hu Y, Yang W, Wei W, Sun Z, Wu B, Li K, Li Y, Zhang Q, Xiao R, Hou C, Wang H. Phyto-inspired sustainable and high-performance fabric generators via moisture absorption–evaporation cycles. *Sci Adv.* **2024**;10:eadk4620.
 202. Kabutey FT, Zhao Q, Wei L, Ding J, Antwi P, Quashie FK, Wang W. An overview of plant microbial fuel cells (PMFCs): configurations and applications. *Renew Sust Energy Rev.* **2019**;110:402.

Publisher's Note Springer Nature remains neutral with regard to jurisdictional claims in published maps and institutional affiliations.

Springer Nature or its licensor (e.g. a society or other partner) holds exclusive rights to this article under a publishing agreement with the author(s) or other rightsholder(s); author self-archiving of the accepted manuscript version of this article is solely governed by the terms of such publishing agreement and applicable law.